PET Evaluation of the Dopamine System of the Human Brain

Nora D. Volkow, Joanna S. Fowler, S. John Gatley, Jean Logan, Gene-Jack Wang, Yu-Shin Ding and Stephen Dewey
Medical and Chemistry Departments, Brookhaven National Laboratory, Upton, New York and Department of Psychiatry, SUNY-Stony Brook, Stony Brook, New York

Dopamine plays a pivotal role in the regulation and control of movement, motivation and cognition. It also is closely linked to reward, reinforcement and addiction. Abnormalities in brain dopamine are associated with many neurological and psychiatric disorders including Parkinson's disease, schizophrenia and substance abuse. This close association between dopamine and neurological and psychiatric diseases and with substance abuse make it an important topic in research in the neurosciences and an important molecular target in drug development. PET enables the direct measurement of components of the dopamine system in the living human brain. It relies on radiotracers which label dopamine receptors, dopamine transporters, precursors of dopamine or compounds which have specificity for the enzymes which degrade dopamine. Additionally, by using tracers that provide information on regional brain metabolism or blood flow as well as neurochemically specific pharmacological interventions, PET can be used to assess the functional consequences of changes in brain dopamine activity. PET dopamine measurements have been used to investigate the normal human brain and its involvement in psychiatric and neurological diseases. It has also been used in psychopharmacological research to investigate dopamine drugs used in the treatment of Parkinson's disease and of schizophrenia as well as to investigate the effects of drugs of abuse on the dopamine system. Since various functional and neurochemical parameters can be studied in the same subject, PET enables investigation of the functional integrity of the dopamine system in the human brain and investigation of the interactions of dopamine with other neurotransmitters. Through the parallel development of new radiotracers, kinetic models and better instruments, PET technology is enabling investigation of increasingly more complex aspects of the human brain dopamine system. This paper summarizes the different tracers and experimental strategies developed to evaluate the various elements of the dopamine system in the human brain with PET and their applications to clinical research.

Key Words: imaging; neurotransmitters; pharmacology; psychiatric illnesses; neurological illnesses.

J Nucl Med 1996; 37:1242–1256

The dopamine system is involved in the regulation of brain regions that subserve motor, cognitive and motivational behaviors (*1–3*). Disruptions of dopamine function have been implicated in neurological (*4*) and psychiatric illnesses including substance abuse (*5*), as well as on some of the deficits associated with aging of the human brain (*6*). This has made the dopamine system an important topic in research in the neurosciences and neuroimaging as well as an important molecular target for drug development (*4,7,8*).

Dopamine cells reside predominantly in the mesencephalon in three neuronal groups: the retrobulbar, the substantia nigra (SN) and the ventral tegmental area (VTA). Dopamine neurons from the SN project predominantly to the dorsal striatum and are mainly concerned with initiation and execution of movements (*9*). Those from the VTA project predominantly to limbic and limbic-connected regions including nucleus accumbens, orbital and cingulate cortices, amygdala and hippocampus and are involved with reinforcement, motivation, mood and thought organization (*1,10–13*). Dopamine neurons from the retrobulbar area project to the hypothalamus where they regulate hormone secretion from the pituitary (*14*). Dopamine cells in the SN and in the VTA and their major projections are shown in Figure 1.

Dopamine is synthesized in the dopamine neurons where it is stored within vesicles which protect it from oxidation by monoamine oxidase (MAO). Dopamine is released into the synapse in response to an action potential and interacts with postsynaptic dopamine receptors. The concentration of dopamine in the synapse is regulated primarily by its reuptake by the dopamine transporters, to maintain low (nanomolar) steady-state concentrations (*15*). Dopamine is also removed by oxidation by MAO A in neurons and by MAO B in glia which surround the dopaminergic nerve terminals and by catecholamine O-methyltransferase (COMT). Brain dopamine release is regulated by autoreceptor as well as by other neuroanatomically distinct neurotransmitters through interactions with the dopamine neuron (*16*).

PET is an imaging method used to track the regional distribution and kinetics of chemical compounds labeled with short-lived positron-emitting isotopes in the living body (*17*). It was the first technology that enabled direct measurement of components of the dopamine system in the living human brain. Dopamine was labeled with ^{11}C 25 yr ago for the purpose of imaging catecholamine metabolism in peripheral organs such as the adrenals and the heart (*18*). Because dopamine does not cross the blood-brain barrier, however, imaging studies of dopamine in the living brain have been indirect, relying on the development of radiotracers to label dopamine receptors, dopamine transporters, precursors of dopamine or chemical compounds which have specificity for the enzymes which degrade synaptic dopamine (Fig. 2). Table 1 gives the brain concentration and activity of the dopamine-related elements which have been measured with PET. Additionally, through the use of tracers that provide information on regional brain activity (i.e., brain glucose metabolism and cerebral blood flow) and of appropriate pharmacological interventions, it has been possible to assess the functional consequences of changes in brain dopamine activity.

Received Sept. 12, 1995; revision accepted Oct. 18, 1995.
For correspondence or reprints contact: Nora D. Volkow, MD, Medical Department, Bldg. 490, Brookhaven National Laboratory, Upton, NY 11973.

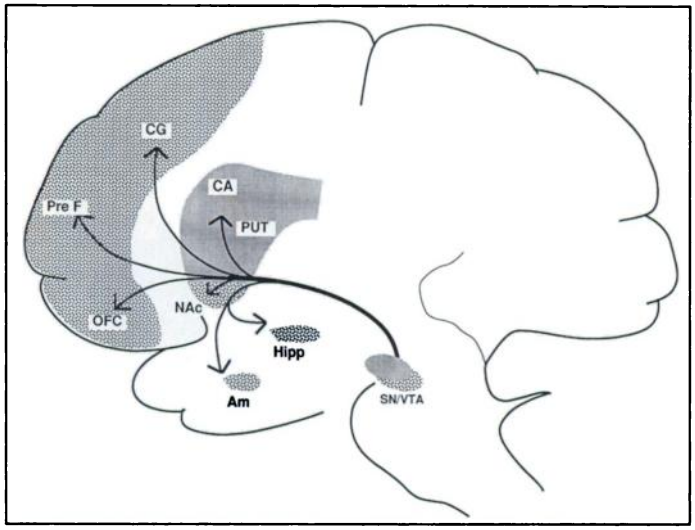

FIGURE 1. Simplified diagram for the dopaminergic projections of the substantia nigra (SN) and the ventral tegmental area (VTA). CG = Cingulate Gyrus, PreF = Prefrontal Cortex, OFC = Orbitofrontal Cortex, NAc = Nucleus Accumbens, CA = Caudate, PUT = Putamen, AM = Amygdala, Hipp = Hippocampus.

This article summarizes the different tracers and experimental strategies developed to evaluate the various elements of the dopamine system in the human brain with PET and their applications in clinical research. Although SPECT methodology can also be used to measure some of the same components (*19*), this chapter will not explicitly discuss this methodology.

TABLE 1
Binding Site Concentrations and Enzymatic Activities in the Human Striatum*

Binding site or activity	Concentration (pmole/g)	Activity (pmole/g/sec)
Receptors		
D1 (*82*)	50	—
D2 (*238*)	20	—
Transporters		
Dopamine transporter (*239*)	400	650†
Enzymes		
Tyrosine hydroxylase (*240*)	—	25
Aromatic L-amino acid decarboxylase (*240*)*	—	200
Monoamine oxidase A (*240,241*)	200	400‡
Monoamine oxidase B (*240*)	200	
Catechol-O-methyltransferase (*242,243*)	—	40§

*Values cited are fairly representative of values reported in other studies of postmortem brains. However, considerable variation is found in the literature, associated with differences in methodologies and in individual subjects. A detailed review of in vitro studies is far beyond the scope of this article. Since enzymatic activities are usually measured with saturating substrate concentrations, the cited values probably do not reflect metabolic fluxes in vivo.

†Determined in rat striatum.

‡Combined MAO A and MAO B activities assayed using tyramine as substrate.

§Determined in human cerebral cortex.

DOPAMINE RECEPTORS

Dopamine receptors are present both pre- and postsynaptically at dopaminergic synapses (Fig. 2). At the postsynaptic side they function in cell-to-cell communication, and at the presynaptic side they modulate the release and synthesis of dopamine (*16*). The dopamine receptors have been the main therapeutic targets in the treatment of psychotic symptoms in schizophrenics and of extrapyramidal motor symptoms in Parkinson's disease patients (*20*). There are five subtypes of dopamine receptors which are grouped into two major families: those which stimulate adenyl cyclase (D1, D5) and those which inhibit adenyl cyclase (D2, D3, D4) (*21*). The concentrations as well as the locations of these receptors in human brain differ and the most ubiquitous are the D1 (50 pmole/g) and D2 receptors (20 pmole/g). The highest concentration for D1 and D2 receptors occurs in striatum (*22*), where D1 receptors appear to be predominantly expressed by striatal output neurons projecting to the SN; and D2 receptors appear to reside mainly in output neurons projecting to the globus pallidus (*23*). Extrastriatal regions have much lower densities (0.3–4 pmole/g) of D2 (*22,24*) and D1 receptors (*25*). D3 receptors exist in low concentrations (1 pmole/g) in the shell of the nucleus accumbens and in the islands of Calleja (*26*). The concentration of D4 receptors is also very low (2.1 pmole/g tissue) and they are localized in several limbic and cortical regions with relatively lower levels in striatum (*27,28*). D5 receptors are located in limbic areas (*29*). PET tracers to measure D2 and D1 receptors have been developed; however there are currently no specific PET ligands to differentially evaluate D3, D4 and D5 receptors.

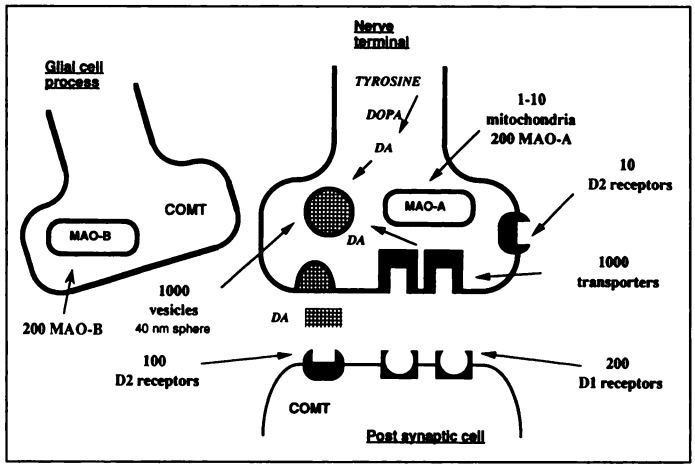

FIGURE 2. Simplified diagram of a typical striatal dopamine synapse. In practice, electron microscopic studies show great structural heterogeneity. There are approximately 10^{11} dopamine terminals per gram of striatum, out of a total number of about 10^{12} terminals per gram. Their average volume is that of a sphere of radius 0.55 μ, and there are about 5000 terminals per striatal cell. The spontaneous firing rate of dopamine cells is about 3 Hz. The volume of each synaptic cleft is about 10^{-17} l, and the total dopamine cleft volume is about 1 μl per gram. The average distance between clefts is about 2 μ. For convenience, D1 and D2 receptors are shown on the same postsynaptic cell, whereas they are almost certainly localized on different cells.

The D2 receptors were the first to be imaged with PET (*30–33*). Several D2 receptor antagonists have been labeled for use with PET (*34*). These ligands differ with respect to their affinity for the D2 receptors, their specificity and their kinetics (Table 2). More recent studies have started to focus on labeling dopamine receptor agonists (*34*). The most widely used D2 PET ligands are the dopamine receptor antagonists [^{11}C]raclopride (*33*) and [^{11}C] or [^{18}F]-labeled N-methylspiroperidol (NMS) (*30,31*). Raclopride is a ligand with moderate affinity for D2 receptors (Kd = 1000–2000 p*M*) (*35*). It has a high selectivity in terms of affinity for receptors for other neurotransmitters but also binds to D3 receptors. NMS has a higher affinity for D2 receptors than raclopride (Kd = 50–300 p*M*) but it also binds to 5HT2 as well as D4 receptors (*27*). Because the

TABLE 2
Radioligands for Dopamine Receptors

Radioligand	Ki in vitro (nm)	Human data ST/CB	Human data Time max (min)	Rodent data ST/CB	Rodent data Time max (min)
D1					
SCH 23390 (*244,245*)	0.3	3		9	20
NNC 756 (*244,49*)	0.17	5	30–60		
NNC 112 (*34*)		8–12			
D2					
Raclopride (*246,247*)	1.1	4	20–40	7	5
NMS (*60,168,247*)	0.05	12	>500	10	>60
IBZM (*78,248–250*)	0.45	1.6		6	
Epidepride (*249*)	0.06	>10	>200	20	120

dissociation of NMS at the 5HT2 receptors is significantly faster than at the D2 receptors, tracer kinetic modeling differentiates these two components of NMS binding (*36*). Since the ratio of D2/(D3 + D4) receptor binding is quite high in most brain regions (*37,38*) the PET measurements from these two tracers predominantly reflect binding to D2 receptors. Also their binding, at least for NMS, appears to be predominantly to postsynaptic receptors (*39,40*). For most PET studies D2 receptor measurements have been limited to the striatum where neurons containing D2 receptors are predominantly GABAergic or cholinergic.

The use of PET to measure D2 receptors in areas other than striatum has been limited by the relatively low concentration of D2 receptors in extrastriatal regions as well as the small volumes of some of the areas (*41*). Although D2 receptors in extrastriatal areas have been imaged with PET and SPECT (*41–44*), the limited sensitivity of these instruments do not allow accurate quantification. The development of D2 ligands with higher affinity for D2 receptors and of PET instruments with a higher sensitivity and spatial resolution may enable improved quantitation of D2 receptors in extrastriatal areas. Some ligands with very high affinity for D2 receptors have recently been developed that may facilitate these measurements. Imaging of the human brain with one of these high affinity ligands [^{11}C]FLB457 (Kd = 20 p*M*), showed significant accumulation in thalamus, substantia nigra, colliculus and temporal cortex (*41,45*).

Initially the development of D2 ligands was targeted towards tracers with very high affinity for D2 receptors. However, tracer kinetic modeling of these tracers is limited by tracer delivery which makes them sensitive to cerebral blood flow (CBF) in addition to receptor concentration (*46*). This is particularly problematic for areas of high receptor concentration since binding equilibrium is not reached within the time period when the measurements can be made. However, these tracers may be useful to quantify D2 receptors in areas with relatively low D2 concentrations as discussed for [^{11}C]FLB457. On the other hand, recent interest in the development of tracers with lower affinities has been stimulated by the feasibility of using them to measure relative changes in synaptic dopamine concentration.

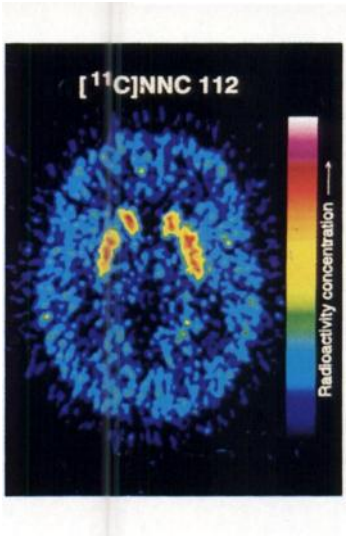

FIGURE 3. Brain images obtained with the D1 receptor radioligand [^{11}C]NNC 112 (*50*) in a healthy control. The image corresponds to the average activity obtained between 9 and 68 min (courtesy of Halldin and collaborators).

The D1 receptors have also been measured with PET though they have been much less investigated. Several D1 receptor antagonists have been labeled with positron emitters and include [^{11}C]SCH 23390 (*47*), [^{11}C]SCH 39166 (*48*), [^{11}C]NNC 687, [^{11}C]NNC 756 (*49*) and NNC 112 (*50*) (Table 2). A problem for most of these radioligands is that they also have considerable affinity for 5HT2 receptors (*49*). [^{11}C]SCH 23390 has been the most widely used (*25*). High uptake of these radioligands occurs in striatum which is the area with the highest D1 receptor density (*25*). The concentration of D1 receptors in cortex is relatively low but is higher than that for D2 receptors (*25*) and has been measured with PET. Of the PET D1 radiotracers the one that gives the highest cortical to cerebellar ratios (1.8–2.2) is [^{11}C]NNC 112 which makes it probably the best of the D1 radiotracers for extrastriatal imaging (Fig. 3) (*34*). The dopamine D1 receptor agonist SKF 75670 was labeled with ^{11}C and proposed as a ligand that may be potentially useful for measuring high-affinity D1 receptor sites (*51*).

Radioligands for D1 and D2 receptors have been used to investigate their involvement in aging, in psychiatric and neurological illnesses and to assess receptor occupancy by antipsychotic drugs. Of the brain changes associated with aging, those in the dopamine system are among the most conspicuous and are probably responsible for some of the motor and behavioral changes in the elderly. PET studies evaluating the effects of age on D2 receptors have consistently reported a significant decline in D2 receptors with age. The estimates for D2 losses obtained from PET studies range between 4–8% per decade of life (*52–55*) and are slightly higher than those reported for postmortem studies which range between 2–5% per decade (*56*). Dopamine D1 receptors in striatum and frontal cortex have also been found to decrease with age (*57*).

Increased brain dopamine activity is an important contributor to the symptomatology observed in schizophrenic patients (*8*). PET studies in schizophrenic patients measuring D2 receptors have yielded inconsistent results with some studies reporting elevations, others no changes and others documenting elevations in some patients but not in others (*41*). Several reasons have been given for these discrepancies related to differences in choice of tracers and subject populations (*58*), including the suggestion that the elevations observed with NMS could be due to increases in D4 receptors in schizophrenic patients (*27*). Studies in schizophrenic patients have also been done to assess the relationship between receptor occupancy by antipsychotic drugs and therapeutic efficacy. For typical neuroleptics it was estimated that 70–80% of the D2 receptors need to be occupied for therapeutic efficacy and that higher occupancies are asso-

TABLE 3
Radioligands for Dopamine Transporters

Radioligand	Ki in vitro[a] (nm)	Peak ST[g] (nCi/cc/mCi)	Human data ST/CB[f]	Human data Time max[b] (min)	Human data Bmax/Kd'[c] (ml/g)	Rodent data ST/Pl[d]	Rodent data ST/CB[f]	Rodent data Time max[b] (min)
RTI-55 (*90,251*)	1.5	130 (500')	12+	>1200	6.7[i]	250	10+	120
WIN 35 428 (*10,93*)	12	150 (60')	4+	>120	5	?	4	60
dtMP (*96,252*)	40	100	2.3	30–40	1.6	25	2	15
Nomifensine (*84*)	45	85[h]	1.9	20–30	0.9[e]	10[e]	—	—
Cocaine (*86,209,253,254*)	100	85	1.7	5–7	0.6	4	1.5	5

[a]Rat striatal membranes.
[b]Time of maximum uptake in striatum.
[c]Calculated using the ratio of distribution volume (DV) in striatum to that in reference tissue, obtained using graphical (*209*) for cocaine and dtMP; Bmax/Kd from two-compartment model for nomifensine; calculated as k_3/k_4 from three-compartment model for WIN 35,428 and RTI-55.
[d]At time of maximal striatal binding; not corrected for plasma protein binding.
[e]Metabolite correction based on plasma/erythrocyte partitioning.
[f]Maximum value observed; at end of measurement period if followed by +.
[g]Representative radioactivity concentration in striatum (nCi/cc/mCi injected) at peak or at indicated time after injection.
[h]Estimated from MBq (g tissue)-1/MBq (g body wt)-1.
[i]Termed V3, or equilibrium partition coefficient (*251*).

ciated with side effects (80–90%) (*59–60*). In contrast, for atypical neuroleptics, such as clozapine, the average D2 occupancy was significantly lower and ranged between 20–67% (*61*). Levels of D2 receptor occupancy by typical neuroleptics were linearly related to drug plasma concentrations (*62,63*). For D1 receptors, levels of occupation by typical neuroleptics ranged between 16–44% and occupation by atypical neuroleptics ranged between 36–59% (*59*). These findings may suggest that D2 receptors are a main target for typical but not for atypical neuroleptics. Though for the atypical neuroleptics, blockade of D1 receptors is larger than that of D2 receptors, therapeutic efficacy may also involve blockade of D4 and 5HT2 receptors (*64*). Studies done to determine if the lack of therapeutic response seen in nonresponding schizophrenic patients was a result of inadequate D2 receptor blockade by the antipsychotic drug showed that there were no differences in receptor blockade by neuroleptics in responders and nonresponders patients (*65–66*). However, the two groups of patients differed in their baseline D2 receptor measures suggesting that there may be underlying biological differences that may predict responsiveness to antipsychotic agents (*62*). These findings also question the common practice of increasing antipsychotic doses beyond the therapeutic window in nonresponding patients.

The dopamine system has been linked with addictive disorders. Imaging studies have shown significant reductions in D2 receptor availability in cocaine abusers which persist after cocaine withdrawal and which were correlated with self ratings of dysphoria (*67,68*). Abnormalities in D2 receptor measures have also been documented in alcoholics (*69*). No drug abuse studies have been done with PET D1 radioligands.

In psychotic depressed patients increases in striatal D2 receptors were recently reported. Because the relation was between D2 and psychosis and not mood this finding was interpreted as most likely reflecting the psychotic state rather than the mood abnormality (*70*). Studies with the D1 receptor ligand [^{11}C]SCH 23390 in depressed patients showed reductions in the binding potential in frontal cortex but no changes in striatum (*71*). These findings provide further evidence that the dopamine system may be involved in affective disorders (*72,73*).

Studies with Parkinson's disease patients have shown that while there may be initial increases during early stages of the disease, for the most part D2 receptor concentrations do not differ from those of age-matched controls (*74–77*). Because L-DOPA requires the presence of dopamine receptors in order to exert a therapeutic effect, imaging with D2 receptors has been used to predict responsiveness in patients with movement disorders (*78*). In patients with Huntington's chorea, where the pathology is localized in striatal neurons, significant reductions in striatal D2 (*79–81*) and D1 (*82*) receptors have been documented. Furthermore, because Huntington's disease affects predominantly medium-sized spiny neurons in striatum, where D1 receptors are located, it has been suggested that D1 ligands may be more sensitive than D2 ligands in detecting degeneration in this disease (*82*). There is also some evidence of reductions in D1 receptors in the frontal cortex of patients with Huntington's chorea (*82*).

DOPAMINE TRANSPORTERS

Interest in the dopamine transporter (DAT) has been stimulated, in part, by the fact that it constitutes the main target site for the reinforcing properties of cocaine (*83*). Additionally, because transporters are localized on the presynaptic terminal they serve as markers of dopamine neurons. Several radioligands have been developed for their suitability as PET and SPECT probes of the DAT. These include [^{11}C]nomifensine (*84–85*), [^{11}C]cocaine (*86*), [^{18}F] GBR 13119 (*87,88*), [^{18}F] GBR 12909 (*89*), [^{11}C] and [^{123}I]RTI-55 (*90, 91*), [^{11}C]WIN 35428 (*92–94*), [^{11}C]methylphenidate (*95*) and [^{11}C]d-threo methylphenidate (*96*). These radioligands differ with respect to their affinities for the DAT, their specific-to-nonspecific binding ratios and their specificity for the DAT as well as their kinetics. Table 3 summarizes this information for DAT ligands which have been examined in reasonable detail in human subjects. The cocaine analogs WIN 35,428 (also known as CFT) and RTI-55 (also known as β-CIT), have affinities for the DAT approximately 10 and 100 times higher, respectively, than those of cocaine and S-(+)-nomifensine and d-threo-methylphenidate have affinities intermediate between those of cocaine and WIN 35,428. Their times to maximum uptake vary by a factor of over 200, that is between about 6 min for cocaine, and

over 1200 min for the high-affinity cocaine analog RTI-55. The initial uptake in brain for the five radioligands in Table 3 is high and corresponds to approximately 7–10% of the injected dose.

Carbon-11-nomifensine was the first DAT ligand developed for PET (*97*). Its uptake in brain is relatively fast and peak concentrations are achieved approximately 20 min after administration which allows for proper modeling and quantification (*84*). A potential disadvantage of this ligand is that it binds more tightly to the norepinephrine transporter than to the DAT. Carbon-11-cocaine exhibits faster kinetics than [^{11}C]nomifensine, with a half-life in striatum of approximately 20 min. Though in vitro studies show binding of cocaine to serotonin as well as norepinephrine transporters, as a PET ligand it shows specificity of binding to DAT (*98*). A limitation for this tracer is that its specific-to-nonspecific binding ratio is relatively low and that its fast kinetics limit the statistical quality of PET images. The specific binding of [^{11}C]methylphenidate and of [^{11}C]d-threo methylphenidate in the brain is mainly due to DAT. Its clearance is slower than that of [^{11}C]cocaine which is an advantage for kinetic analysis in that it is fast enough to allow for proper quantification but is slow enough to permit appropriate counting statistics. A disadvantage of racemic [^{11}C]methylphenidate when compared with [^{11}C]d-threo methylphenidate is that the *l* enantiomer in the racemic mixture contributes to nonspecific binding and confounds its quantification. An advantage for [^{11}C]d-threo methylphenidate and for [^{11}C]methylphenidate is that its pharmacology in humans is well studied so that unlabeled methylphenidate can be administered to humans to assess nonspecific binding.

RTI-55 has highly desirable properties which are optimized in the ^{123}I-labeled compound used with SPECT (i.e., very high affinity for the DAT and a high specific-to-nonspecific binding ratio) (*90*). The SPECT measurements with [^{123}I]RTI-55 are made when the radioligand distribution corresponds to an equilibrium situation, which is thought to be the case after about 18 hr. However, PET measurements with [^{11}C]RTI-55 (half-life = 20 min) must be conducted very far from equilibrium (*91*). A danger under these conditions is that tissues with some threshold concentration of binding sites may trap essentially every molecule of radiotracer which is delivered. This is expected to diminish the sensitivity of radiotracer binding to small decreases in binding site concentration. Furthermore, radiotracer binding will become more sensitive to alterations in tissue perfusion, which proportionately alters delivery of radioligand. Carbon-11-WIN 35,428 also does not achieve a maximum value of striatal binding within the time constraints of PET experiments; its striatal uptake is still rising after more than 5 half-lives for ^{11}C have elapsed (110 min) (*93*). The extent to which this may compromise its ability to detect small decreases in DAT concentration, or its usefulness in circumstances of altered CBF, is presently unclear. PET studies are required to determine under what circumstances one DAT ligand may be more accurate than another. For example, under conditions of decreased DAT availability and/or to examine regions with low DAT densities, ligands with very high affinities such as [^{11}C]WIN 35428 may be desirable. However, for quantification in patients with decreased CBF, ligands with a relatively lower affinity for the DAT such as [^{11}C]d-threo methylphenidate may be more appropriate.

Though most of the radioligands developed for monoamine transporters have been targeted to the cellular transporters, [^{11}C]tetrabenazine has been proposed as a PET ligand to measure the vesicular monoamine transporter (*99*). The advantage for this type of ligand is that it does not appear to up- or down-regulate in response to treatment and hence may be less sensitive to the confounding effects of medication (*100*). The disadvantage is a lack of specificity for the different monoamine transporters.

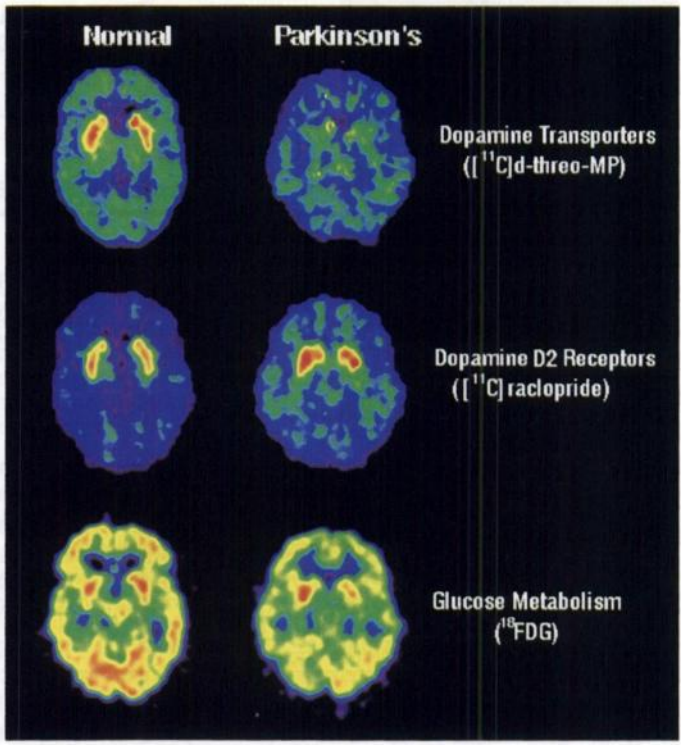

FIGURE 4. Brain images from a multiple tracer study comparing a patient with Parkinson's disease and a control. The images for D2 receptors and for dopamine transporters correspond to the distribution volumes of [^{11}C]raclopride and of [^{11}C]d-threo methylphenidate, respectively. Metabolic images were obtained with ^{18}FDG.

It is to be noted that most studies in humans using DAT radioligands have shown age-related decreases in binding (*85,101,102*) which are consistent with the reduction in DAT and in dopamine cells documented in postmortem studies (*103,104*). In patient populations these radioligands have been used to assess dopamine cell degeneration in subjects with Parkinson disease who show marked reductions in DAT when compared with healthy age-matched controls (Fig. 4) (*85,90,91,94*). Studies in cocaine abusers have shown that while there are increases in DAT shortly after withdrawal (*105*) there are decreases or no changes with protracted withdrawal (*106*). A preliminary study done in violent alcoholics showed significant elevations of DAT when compared with nonalcoholic subjects (*107*). In contrast, nonviolent alcoholics had lower DAT levels than controls (*107*).

DOPAMINE SYNTHESIS

Dopamine synthesis occurs within the dopamine neuron as shown in Figure 5. Tyrosine is transported via amino acid carriers in the blood-brain barrier and cell membranes. Once in the intracellular space it is hydroxylated to L-3,4-dihydroxyphenylalanine (L-DOPA) by tyrosine hydroxylase (TH, E. C. 1.14.16.2). L-DOPA is then decarboxylated by aromatic L-amino acid decarboxylase (AADC, E. C. 4.1.1.28) (*108*) to form dopamine.

TH is the rate-limiting enzyme in the synthesis of brain dopamine. PET radiotracers which would enable an assessment of TH activity are still under development (*109,110*). The first PET tracer developed for studies of dopamine metabolism in the human brain was ^{18}F-labeled fluoro L-DOPA (*111,112*). Like L-DOPA, 6-[^{18}F]fluoro-L-DOPA crosses the blood-brain

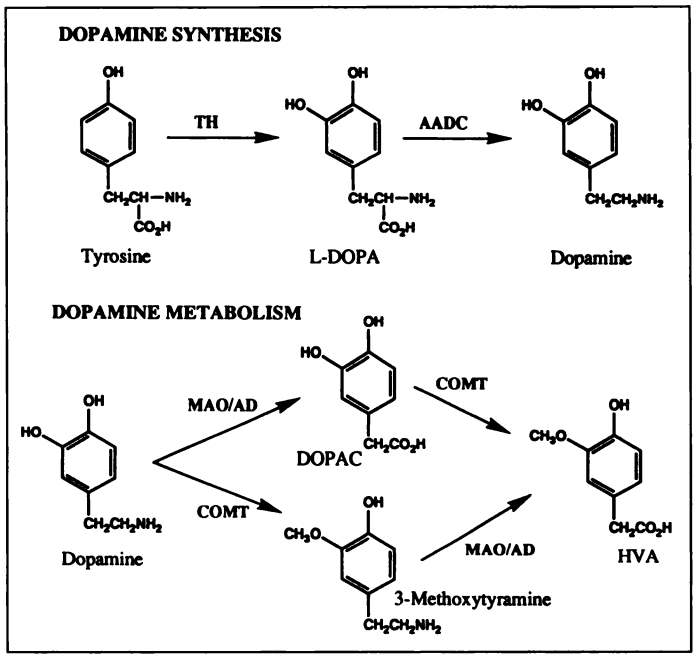

FIGURE 5. Pathways for the synthesis and metabolism of dopamine in the CNS. TH, tyrosine hydroxylase (EC 1.14.16.2); AADC, aromatic amino acid decarboxylase (EC 4.1.1.28); MAO, monoamine oxidase (EC i.4.3.4); AD, aldehyde dehydrogenase (EC 1.2.1.3); COMT, catechol-O-methyltransferase (EC 2.1.1.6).

barrier resulting in an accumulation of ^{18}F in striatum. This striatal accumulation appears to be unidirectional over the first 90 min and probably reflects the synthesis of fluorodopamine and subsequent storage within vesicles (*113*). However, because L-DOPA (and fluoroDOPA) and its metabolites are extensively metabolized by MAO and by COMT, labeled metabolites, especially 3-O-methyl-6-[^{18}F]fluoroDOPA also contribute to striatal ^{18}F activity as visualized by PET (*114*). This complicates the estimation of indices which reflect the rate of dopamine synthesis. To minimize the extensive peripheral metabolism of fluoroDOPA by AADC, which limits tracer availability in brain, peripheral AADC inhibitors have been used to spare [^{18}F]fluoroDOPA (*115*). Unfortunately, AADC blockade enhances COMT-catalyzed formation of peripheral [^{18}F]3-O-methylfluoroDOPA which enters the brain and contributes to the nonspecific signal.

It has been suggested that the accumulation of 6-[^{18}F]fluoro-L-DOPA metabolites in the striatum parallels AADC activity and that this reflects the brain's capacity for dopamine synthesis (*116*). A recent PET study using 6-[^{18}F]fluoro-L-DOPA employed a kinetic model that took into account labeled metabolites to calculate the relative rates of conversion of 6-[^{18}F]fluoro-L-DOPA to 6-[^{18}F]fluorodopamine. The highest values for AADC activity were found in caudate and putamen which are consistent with in vitro measurements.

The extent to which 6-[^{18}F]fluoro-L-DOPA parallels the behavior of L-DOPA has been addressed by comparing 6-[^{18}F]fluoro-L-DOPA and either [β-^{11}C]L-DOPA, [β-^{11}C]6-fluoro-L-DOPA or [^{3}H]L-DOPA (*117,118*). The behavior of 6-[^{18}F]fluoro-L-DOPA qualitatively parallels that of L-DOPA but its uptake is higher and its metabolism by COMT is faster. The brain kinetics of L-[β-^{11}C]DOPA have been measured in human volunteers with PET (*119*). The use of [β-^{11}C]L-DOPA allows PET studies to be carried out at tracer conditions even though its use was reported to be limited by large statistical variation due to the limited time frame for quantitation of low radioactivity. Recently this tracer has been applied in the study of dopamine metabolism in patients with unipolar depression (*120*).

The accumulation of ^{18}F after the injection of 6-[^{18}F]fluoro-L-DOPA has been used as a measure of the integrity of the nigrostriatal dopamine system in Parkinson's disease (*7*) and a recent postmortem study has correlated fluoro-DOPA uptake constants with nigrostriatal neuronal density (*121*). The extent to which ^{18}F accumulation is sensitive to smaller age-related losses in dopamine neurons is controversial with some investigators finding an age-related loss in dopamine neurons is controversial with some investigators finding an age-associated decline and others finding no change in PET studies of normal subjects (*122–124*). Studies in the postmortem human brain suggest that AADC may be up-regulated in dopamine neurons that are spared during aging and that PET measures of 6-[^{18}F]fluoro-L-DOPA uptake may overestimate the number of dopamine nerve terminals during normal aging (*125*).

In patients with Parkinson's disease, a correlation has been found between 6-[^{18}F]fluoro-L-DOPA uptake in putamen and motor deficits and between 6-[^{18}F]fluoro-L-DOPA uptake in caudate and memory (delayed recall test) (*126*). Though most studies done with 6-[^{18}F]fluoro-L-DOPA measure AADC activity in striatum, concentrations in the amygdala, mesencephalon, hippocampus and thalamus are higher than those in the cerebellum (*116*).

Other tracers have been developed in an attempt to improve quantitation and to reduce the spectrum of labeled metabolites from 6-[^{18}F]fluoro-L-DOPA. The best characterized is [^{18}F]fluoro-m-tyrosine which is missing the hydroxyl group on carbon-4 of the aromatic ring (*127,128*). This molecule is a substrate for AADC but is not a substrate for COMT. This tracer has been investigated in monkeys and showed low peripheral metabolism as predicted (*118*). Initial studies have been carried out in humans and it has been proposed that the use of labeled fluoro-m-tyrosine will be a considerable advance over the use of labeled fluoro-DOPA for the measurement of AADC activity (*129*). Another tracer, [^{18}F]fluoro-β-fluoromethylene-m-tyrosine is also being investigated (*130*).

DOPAMINE METABOLISM

Monoamine oxidase (MAO, EC 1.4.3.4) formally oxidizes amines such as dopamine to the corresponding aldehyde (*131*). The enzyme exists in two subtypes, MAO A and MAO B (*132*). Though both forms can oxidize each of the biogenic amines, MAO A preferentially oxidizes 5-hydroxytryptamine whereas MAO B oxidizes benzylamine. Dopamine is a substrate for both subtypes of MAO (*133*), and both subtypes have similar affinities for dopamine (*134*). There are selective inhibitors for each form of the enzyme, the best known of which are clorgyline for MAO A (*135*) and L-deprenyl for MAO B (*136*). In the human brain MAO B predominates (B:A = 4:1) (*137*). Since MAO B is largely compartmentalized in glial cells, it has been suggested that MAO B inhibition spares extraneuronal dopamine (*138*). Many studies support a link between increases in MAO B (but not MAO A) and aging and neurodegenerative disease (*139*).

By far the major medical interest in MAO stems from the neuropsychological effects of MAO inhibitor drugs on the human brain. Indeed, MAO inhibitors were among the first antidepressant drugs. The fact that MAO inhibition spares brain dopamine led to the use of the MAO B inhibitor L-deprenyl as an adjunct with L-DOPA in the treatment of Parkinson's disease (*140*). More recently it has been shown that L-deprenyl slows the natural progression of Parkinson's disease (*141*).

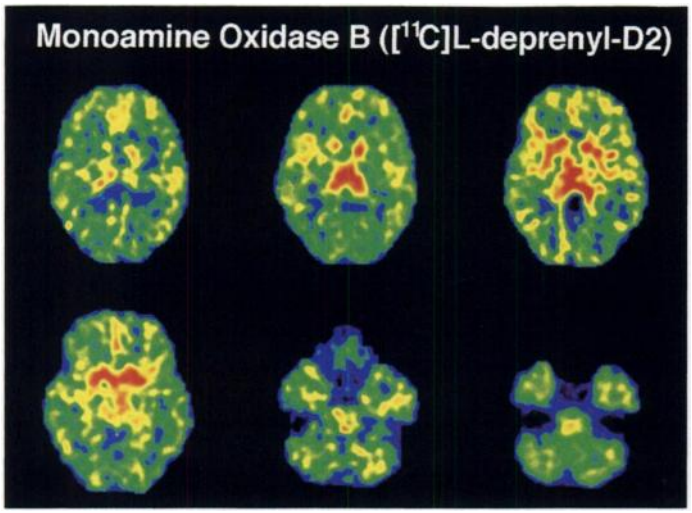

FIGURE 6. Influx constant images of human brain MAO B using [^{11}C] H-deprenyl-d2. Notice the high values in the subcortical regions and lower values in cortex in agreement with postmortem assays.

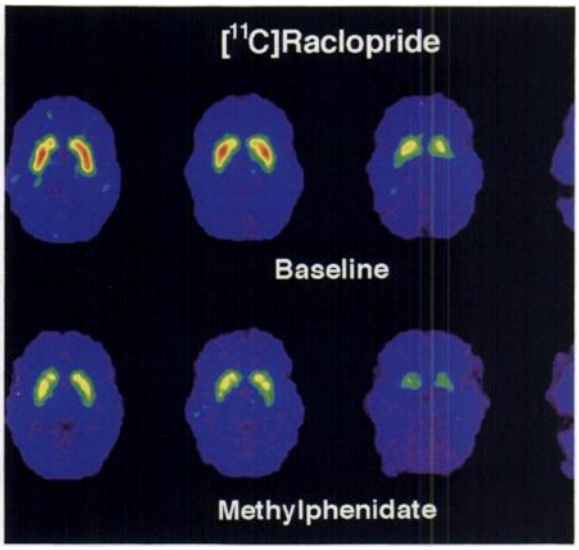

FIGURE 7. Brain images of the distribution volume for [^{11}C]raclopride obtained with no pharmacological intervention and after administration of methylphenidate.

Though there is controversy concerning the mechanism(s) responsible for the therapeutic actions of L-deprenyl (*142*), this finding has stimulated interest in the development of new MAO inhibitor drugs.

PET studies of MAO have measured its regional distribution, its inhibition and its synthesis rate. Two general approaches to mapping MAO with PET in vivo have been developed, one uses the labeled suicide inactivators, L-deprenyl and clorgyline, to label the two forms of the enzyme (*143*) and the other uses labeled dimethylphenethylamine to produce ^{11}C-labeled dimethylamine, a MAO B-generated metabolite which is intracellularly trapped (*144*). The most frequently used approach is the measurement of MAO B with [^{11}C]L-deprenyl and [^{11}C]L-deprenyl-D2 (a deuterium-substituted analog of L-deprenyl with improved sensitivity (*145*)).

The general approach to the in vivo labeling of MAO B with [^{11}C]L-deprenyl is based on the principle of suicide inhibition in which the radiotracer becomes covalently attached to the enzyme as a result of oxidation and the formation of a very reactive intermediate. The distribution of ^{11}C in brain after the injection of [^{11}C]L-deprenyl closely parallels the distribution of MAO B as determined in the postmortem human brain (Fig. 6). Carbon-11-L-deprenyl has been used to determine the duration of MAO B inhibition by pharmacological doses of L-deprenyl. Since L-deprenyl is a suicide inactivator of MAO B, enzyme recovery after withdrawal from the drug requires the synthesis of a new enzyme. PET measurements showed that the half-time for recovery of brain MAO B averaged about 40 days (*146*). Though L-deprenyl is given to patients at a dose of 10 mg/day, it is obvious from the PET study that complete MAO B inhibition can be obtained at a fraction of this dose. A similar investigation was carried out to study the duration of MAO B inhibition by the new reversible, MAO B inhibitor drug Ro 19 6327 (*147,148*) which is being proposed for the treatment of Parkinson's disease. This study showed total recovery of the enzyme after 36 hr of Ro 19 6327 discontinuation.

Catechol-O-methyltransferase (COMT; EC 2.1.1.6) is one of the two major enzymes which metabolize dopamine (*149*). COMT catalyzes the transfer of a methyl group from S-adenosyl-L-methionine to the phenolic group of a substrate that must have a catechol structure. It is distributed throughout the body and brain and is an important molecular target in the development of drugs to treat Parkinson's disease (*150*). The product of dopamine metabolism by COMT is 3-methoxytyramine and the concentration of this compound in the brain is taken as an index of dopamine release (*151*). Although the main function of COMT was described in the late 1950s (*152*), the significance of this enzyme has been less studied, in part, because of the lack of suitable in vivo inhibitors. The recent development of selective and potent COMT inhibitors (*150*) has presented the opportunity to investigate the distribution of COMT in the living body with PET and appropriately labeled COMT inhibitors. In this regard Ro 41-0960 (3,4-dihydroxy-5-nitro-2′-fluorobenzophenone), a potent and selective fluorine-containing COMT inhibitor which has been reported to cross the blood-brain barrier, has been labeled with ^{18}F in order to study brain COMT with PET (*153*). Though PET studies in the baboon using ^{18}F-labeled Ro 41-0960 demonstrated a negligible uptake in the brain, high uptake was observed in the kidneys and in other organs known to have high COMT activity demonstrating the potential of PET to investigate peripheral, if not central, COMT activity (*154*).

DOPAMINERGIC RESPONSIVITY AND DOPAMINE RELEASE

The competition of endogenous dopamine with D2 receptor radioligands presents the opportunity to measure changes in synaptic dopamine in vivo by observing the degree of change in the binding of a D2 receptor radiotracer by a pharmacological challenge or other perturbation (*155*). The in vivo striatal binding of [^{3}H]raclopride has been shown to be sensitive to pharmacologically-induced changes in endogenous dopamine (*35,156*). This property in turn has been used to assess changes in endogenous synaptic dopamine concentration with PET with labeled raclopride and with labeled NMS (*157–162*). Comparisons are made between the binding of the radiotracer at baseline and after administering a drug that changes dopamine concentration (i.e., methylphenidate, amphetamine) (Fig. 7). Studies in humans have shown that methylphenidate significantly reduced [^{11}C]raclopride binding in the brain. The reductions varied among subjects and decreased with age (*160*). Because [^{11}C]raclopride binding is highly reproducible (*163–164*) these reductions most likely reflect changes in synaptic dopamine. The effects of amphetamine on dopamine release in the human brain have also been measured with SPECT and the D2 radioligand [^{123}I]IBZM (*165*).

Investigating relative changes in dopamine concentration in

response to a drug provides a tool with which to evaluate the relationship between drug-induced changes in dopamine concentration and its behavioral effects (*160,165*). It may also enable the detection of dopamine dysfunction with a higher sensitivity than when studying patients during baseline conditions. Limitations of this strategy are: the inability to measure baseline dopamine concentration; the limited spatial resolution of PET (measures are of large volumes of tissue which may be heterogeneous in their responses to drugs); the inability to differentiate whether changes in binding reflect the magnitude of the rise in dopamine or the ratio of high- versus low-affinity D2 receptors (dopamine predominantly competes with the radiotracers for the binding to high-affinity D2 receptors); and the relatively low sensitivity of the technique which requires the use of pharmacological challenges that raise dopamine levels severalfold. Also, because the pharmacological challenge can affect tracer delivery (*166*), studies are required to assess its effects on tracer kinetics and on the model parameter. In the case of [^{11}C]raclopride, the model parameter used (Bmax/Kd) is insensitive to changes in CBF (*167*). To our knowledge, the sensitivity of these strategies to nonpharmacological, i.e., behavior-related (*168*) changes in dopamine has not been demonstrated. This methodology differs from the measures obtained with microdialysis (*169*) in that it simultaneously measures all brain regions, it measures predominantly synaptic rather than extracellular dopamine concentration, and it is minimally invasive permitting its use in awake human subjects.

Recent studies in our laboratory using electrically-stimulated brain slices have suggested that the binding of D1 radioligands may be more sensitive to changes in synaptic dopamine than to D2 radioligands. To our knowledge this has not yet been evaluated in PET experiments (*170*).

INTERACTIONS OF DOPAMINE WITH OTHER NEUROTRANSMITTERS

Dopamine does not function alone and behaviors that involve dopamine are also regulated by other neurotransmitters (*16*). The dopamine system interacts with several neurotransmitters both in the mesencephalic area and in projection regions. Close interactions between dopamine and norepinephrine, serotonin, gamma-amino butyric acid (GABA), glutamate, acetylcholine, opiates and CCK among others, have been documented (*16*). These interactions regulate dopamine function and are of relevance for understanding brain pathology as well as for the therapeutic drug development. For example, interactions of dopamine with glutamate have been associated with schizophrenia (*171*) and Parkinson's disease (*23*); those with serotonin with schizophrenia (*172*) and those with the opiate system with substance abuse (*173*). Understanding how the dopamine system is modulated by other neurotransmitters is leading to the development of candidate drugs which exploit these interactions, e.g., glutamate antagonists for Parkinson's disease (*174*) and serotonin antagonists in schizophrenia (*175*).

The feasibility of studying neurotransmitter interactions with PET was first demonstrated in the baboon brain for the interaction between dopamine and acetylcholine (*176*). The methodology takes advantage of the sensitivity of receptor-specific radioligands to competition with endogenous neurotransmitters in an analogous way to the strategy described to measure dopamine responsivity. The difference is that instead of changing dopamine concentration with a drug that directly interacts with dopamine neurons, it uses drugs which affect specific neurotransmitters that are known to modulate dopamine (*158*). Using this strategy PET has been used to evaluate the ability of acetylcholine (*176,177*), GABA (*157*), serotonin (*178*) and the opiate system (*179*) to modulate striatal dopamine release. In humans the interactions between dopamine and acetylcholine have been investigated in healthy controls (*177*). Striatal dopamine D2/acetylcholine interactions have also been studied in primates using [^{18}F](−)-4-N-ethyl-fluoroacetamidobenzovesamicol as a radioligand marking cholinergic activity (*180*).

The possibility that abnormal interactions between cortical glutaminergic neurons and the striatal dopamine system may underlie schizophrenia was also recently investigated with PET where it was demonstrated that DOPA decarboxylase activity is elevated in patients with psychosis as measured with 6-[^{18}F]fluoro-DOPA (*181*). This observation was interpreted as supporting the hypothesis that in schizophrenia, psychosis is the result of insufficient cortical (glutamatergic) stimulation of nigrostriatal terminals leading to a low baseline concentration of extracellular dopamine in the striatum and a corresponding increase in the activity of the enzymes involved in dopamine synthesis (*182*).

REGIONAL BRAIN GLUCOSE METABOLISM AND CBF

Brain metabolism is tightly coupled with brain function and it can therefore be used to assess the regional functional changes associated with manipulation of the dopamine system. Local brain metabolic rates can be measured using FDG (*183*). Though a number of energy-requiring processes contribute to the basal rate of glucose utilization, it is neuronal activity which is the major contributor to glucose utilization (*184–186*). Under physiological conditions CBF is tightly coupled to glucose metabolism so that it can also be used as an index of brain function. However, care must be taken when measuring CBF as a functional tracer in experiments that use pharmacological challenges since some of the psychoactive drugs have vasoactive properties (*166*). In humans, manipulations of the dopamine system have been made using drugs that raise dopamine concentration and with drugs that block D2 receptors. For the most part, drugs that increase dopamine concentrations (i.e., cocaine and amphetamine) when given acutely have been shown to produce a widespread decrease in brain glucose metabolism (*187,188*). Acute administration of D2 receptor antagonists was shown to have a minimal effect on regional brain glucose metabolism in schizophrenic patients (*189*). In contrast, acute haloperidol administration in normal subjects decreased metabolism in frontal and limbic cortices, in thalamus and in caudate nucleus (*190*). Though not always consistent, most studies evaluating the effects of chronic treatment with D2 receptor antagonists have shown increases in striatal metabolism and relative decreases in frontal metabolism (*191–198*). The inability to differentiate changes in metabolism that result from direct changes in dopamine levels from those which reflect secondary adaptation processes limits the interpretation of these findings.

MULTIPLE TRACERS STUDIES

The relatively low dosimetry from positron-labeled tracers permits injection of volunteers with more than one PET radiotracer. Multiple tracer studies that measure glucose metabolism and/or CBF in conjunction with specific dopamine tracers, enable one to assess the functional significance of these dopamine elements. Such studies have been done to investigate the relation between brain glucose metabolism and dopamine D2 receptors in cocaine abusers. A significant correlation was reported between dopamine D2 receptors and glucose metabolism in orbitofrontal cortex, cingulate gyrus and superior frontal cortex (*68*). Lower values for D2 receptor concentration are

associated with lower metabolism in these brain regions. In Parkinson's disease studies that evaluated in the same subject 6-[^{18}F]fluoroDOPA and brain glucose metabolism have also reported an association between the decreases in [^{18}F]DOPA uptake in striatum and decreases in metabolic activity in frontal cortical areas (*199,200*). Multiple tracer studies also enable investigation of the relationship between the different elements of the dopamine system and may aid the evaluation of patients. An example of such a study is shown in Figure 4 from a Parkinson's disease patient who was evaluated with three tracers: [^{11}C]d-threo methylphenidate for DAT; [^{11}C]raclopride for D2 receptors; and FDG for regional brain glucose metabolism. While this patient showed marked reductions in DAT and in frontal metabolic activity; there were no differences in dopamine D2 receptors. The DAT/D2 ratio was therefore markedly reduced when compared with that of controls. The use of multiple tracers is slowly starting to emerge as a powerful tool to investigate the relations between functional and neurochemical parameters in the normal and the diseased brain.

QUANTITATIVE MEASURES OF DOPAMINE PARAMETERS WITH PET

The models used to describe the uptake and binding of PET ligands are generally simple two- or three-compartment models with at most four kinetic parameters even though the physiological processes underlying the PET image are complex and involve, among other factors, delivery via capillary network, diffusion to the binding site, competition with endogenous neurotransmitter, binding to plasma proteins and association and dissociation with specific binding sites (of possibly more than one kind). The models used are simply of necessity since there are only two measurements: plasma radioactivity due to the labeled ligand and the radioactivity measured by the PET camera which is the total radioactivity due to all processes occurring within the voxel. As a result only a limited number of model parameters can be uniquely determined (*201*). Three-compartment models for D2 dopamine receptors have been proposed (*33,46,202–206*). Alternatively there are model-independent methods for the analysis of PET data which do not depend upon a particular model but only require that linear first-order kinetics are applicable to the movement of the radiotracer (*207–210*). Both approaches provide some measure which is a function of the free receptor concentration.

A radioligand generally can be classified as either reversible when there is uptake and loss of the ligand from tissue during the course of the experiment or irreversible, in which case the ligand is taken up by receptors/enzyme and remains bound for the duration of the experiment. The three-compartment model which has been applied to both types of radiotracers consists of three to four parameters. Two parameters control transport between plasma and tissue, K_1 is the plasma to tissue influx constant and k_2 is the tissue-to-plasma efflux constant. There are one or two receptor parameters, k_3, which is proportional to the number of free receptors or binding sites and k_4, the ligand-receptor dissociation constant (in the case of irreversible ligands $k_4 = 0$) (*33,46,203,206.*) The transport constants, as they are generally used, are functions of blood flow, permeability, plasma protein binding (K_1) and nonspecific binding (k_2). In some models blood flow and nonspecific binding are considered separately (*202*). Values for the model parameters can be determined by fitting the model to PET data or by relying on a pseudo equilibrium to estimate receptor number from PET data directly (*33,204*). There are many different approaches and assumptions used in the determination of the model parameters even within the framework of the three-compartment model (*33,46,202–204*) but the goal is to separate the effects of transport from that of receptor binding. The parameter of interest is $k_3 \alpha$ Bmax or $k_3/k_4 \alpha$ Bmax/Kd where Bmax is the total receptor concentration and Kd is the equilibrium dissociation constant; Bmax/Kd is sometimes referred to as the binding potential (*202*). General aspects of parameter estimation and modeling techniques used in PET have been reviewed (*211–214*).

For reversible ligands, the distribution volume (DV) can be determined directly. The DV is the ratio of tissue radioligand concentration to plasma radioligand concentration at equilibrium.

Alternatives to the methods that require explicit model parameter determination are the model independent methods which are much easier to apply. In the case of irreversibly binding ligands, the graphical technique (Patlak plot) (*207,208*) has been extensively used. In this method a plot of

$$\mathrm{ROI(T)} / \mathrm{Cp(T)} \text{ versus} \int_0^T \mathrm{Cp(t)/Cp(T)}$$

becomes linear after some time with a slope Ki, referred to as the influx constant. Cp(T) is the plasma radioactivity of the labeled ligand and ROI(T) is the tissue radioactivity measured by the PET camera at time T. K_i determines the steady-state rate of transfer of the ligand into the irreversible compartment which is given by K_iCp. K_i, a function of the number of free receptors or binding sites, is also a function of tracer delivery (K_1). In the case of a very high rate of trapping (controlled by k3) $K_i \approx K_1$ and therefore contains little information about free receptor concentration, a situation referred to as flow limited. By reducing the rate of trapping, the sensitivity of K_i to variations in free receptor concentration can be improved. This was done with deuterium-substituted L-deprenyl ([^{11}C] L-deprenyl-D2) for which the trapping rate was reduced over that of L-deprenyl in regions of high MAO B (*145*). Under these conditions Ki is much less sensitive to changes in delivery and more sensitive to changes in enzyme/receptor concentration. The condition of being flow limited is a consequence of the rapid trapping and irreversible nature of the binding and limits the ability to determine reliable measures of free receptors whether expressed in terms of k_3 of the three-compartment model or K_i. The slope of a plot of radioactivity in the receptor region to that in a nonreceptor region versus time as a measure of the number of free receptors has also been used (*46,60*). This method can be derived from the Patlak analysis for irreversibly binding ligands (*46,215*). The steady state (when this ratio becomes constant). Since the DV is a steady-state quantity, it is independent of blood flow (*167,216*). In terms of model parameters the DV is given by

$$\mathrm{DV} = \frac{K_1}{k_2}\left(1 + \sum_i \mathrm{Bmax'}_i / \mathrm{Kd'}_i\right) \qquad \text{Eq. 1}$$

where

$$\frac{\mathrm{Bmax'}_i}{\mathrm{Kd'}_i} = \frac{(\mathrm{Bmax}_i - \mathrm{L} - \mathrm{L'})}{\mathrm{Kd}_i}\left(\frac{1}{1 + \mathrm{NS}}\right). \qquad \text{Eq. 2}$$

Bmax_i is the receptor concentration of receptor type i and Kd_i is the equilibrium dissociation constant, NS refers to the ratio of kinetic constants for nonspecific binding (assumed to be sufficiently rapid that it is always in a steady state (*202*)), L is the concentration of endogenous neurotransmitter and L′ is the concentration of receptors occupied with unlabeled ligand or drug. The free receptor concentration is related to the DV. By

taking the DV ratio of receptor region (ROI) to a nonreceptor region (NR), the dependence upon plasma protein binding which is contained in K_1 is eliminated. It is assumed that the ratio of transport constants is close to the same for both regions.

$$\frac{DV(ROI)}{DV(NR)} - 1 = \sum_i Bmax'_i/Kd'_i. \qquad \text{Eq. 3}$$

There are several methods for determining the DV. One of them involves an infusion protocol to maintain a constant plasma level and the DV is directly determined from the ratio of radioactivity in tissue to that in plasma (*217*). However, for most PET studies the ligand is introduced as a bolus injection which requires a modeling technique to determine the DV. Under these conditions the DV can be determined using a two-compartment two-parameter model that does not explicitly contain receptor parameters (*210*). The DV can also be determined from the plot of

$$\int_0^T ROI(t)\,dt/ROI(T) \text{ vs } \int_0^T Cp(t)\,dt/ROI(T),$$

which becomes linear after some time with a slope equal to the DV (*209*).

The determination of absolute values for the receptor concentration Bmax has been reported for NMS (*218*) and raclopride (*219*), although with conflicting results. Such experiments require a loading dose of unlabeled ligand or drug to reduce the number of available receptors. However, for an ^{18}F-labeled congener of raclopride, the three-compartment model failed to give consistent results for the ligand-receptor dissociation (k_4) under conditions of saturation compared to the high specific activity nonsaturation experiments (*220*). The authors postulate that the geometry of the synapse and the physical arrangement of receptors on the membrane are responsible for the discrepancy. In spite of this failure the three-compartment model has proved to be useful in assessing changes in receptor availability even though it may lack the complexity to reproduce the observed behavior of ligand binding under some circumstances.

FUTURE DIRECTIONS

Radiotracer Design and Development

Advances made in radiotracer design and synthesis have played a major role in shaping the PET field as we know it today. These advances have made it possible to create the radiotracers required to investigate new biomolecular targets and to improve the quantitative nature of PET measurements. Development of more selective radioligands for dopamine receptor subtypes and radiotracers with a range of kinetic properties to maximize information from specific experimental paradigms are important immediate goals. Also, new radiotracers which have the sensitivity to probe small changes in synaptic dopamine, as might be expected to arise from behavioral stimulation, and/or to assess baseline dopamine concentration would also be an important advance in our understanding of the functional activity of the dopamine system.

Functional State of Receptors

The documentation of constitutively active receptors that couple to G proteins without the need of an agonist (*221–224*) has led to the renewed consideration of the two-state receptor model for G-protein coupled receptors (*225*). The two-state receptor model describes an equilibrium between active (R*) and inactive receptors (R) which is perturbed by the presence of receptor ligands; agonists stabilize R* favoring the active state, inverse agonists stabilize R favoring the inactive state and antagonists do not perturb the equilibrium (*225,226*). The presence of constitutively active receptors was recently documented for dopamine D5 receptors (*227*). Though the physiological significance of these constitutive dopamine receptors is not understood there is evidence from other receptor systems that abnormal expression of constitutive receptors can lead to pathology as is the case for mutations in the rhodopsin receptor which lead to retinitis pigmentosa (*228*), and for mutations of the thyrotropin-stimulating hormone receptor which are associated with the presence of oncogenic lesions (*229*). Access to experimental strategies with PET that would enable discrimination of R* from R would allow the assessment of the functional state of the receptors in the normal and the diseased brain. The possibility that there is increased expression of constitutive receptors in diseases with overactivity of the dopamine system, as has been postulated for schizophrenia, merits investigation. The PET strategy described to measure dopaminergic responsivity after a pharmacological challenge could perhaps be useful to assess the functional state of receptors since it reflects not only changes in intrasynaptic dopamine but also the ratio of R* to R for dopamine binds predominantly to R*. Unfortunately this strategy is confounded by baseline measures, since in a state with increased expression of R*, dopamine would also be more effective in blocking binding of the receptor radioligand. Another strategy which has been proposed to measure the functional state of the receptors with PET is to differentially evaluate binding of dopamine receptor agonists from binding of dopamine antagonists (*230*).

Second Messenger Systems

The binding of dopamine to its receptors results in an intracellular response transmitted by second messenger molecules such as cAMP which in turn regulate enzymatic processes within the cell such as protein kinase A (*16*). Changes in second messenger systems will therefore affect the functional effects of the receptors on the cells expressing them and may be involved in disease, i.e., affective disorders (*231*) and drug addiction (*232*). The pharmacological properties of certain therapeutic agents, such as lithium, appear to be in part mediated by their ability to change these second messenger systems (*233*). Development of radiotracers for second messenger systems would be an enormous advance because there are theoretical reasons to expect that brain diseases and therapeutic interventions will express themselves more clearly at the level of second- and third-messenger systems.

Fluorine-18-labeled 1,2-diacylglycerols are currently being investigated as PET ligands to image second-messenger systems (*234*). New tracers targeted to specific elements of the second-messenger systems may allow investigation of their involvement in brain diseases.

Molecular Genetics

Antisense nucleotides are finding applications in many fields and have the potential to map mRNA for various molecular targets including elements of the dopamine system such as receptors and transporters. The antisense nucleotide complements the coding strand of DNA and selectively binds to a strand of specific mRNA. The possibility of using this technique in nuclear medicine has been investigated primarily to permit the evaluation of oncogenes amplified in cancer cells (*235*). Using PET to measure regional expression of mRNA in brain would be predicted to be limited by difficulties in preparation of the required labeled oligonucleotides and delivery of nucleotides into the brain as well as the relatively low rate of trapping and diffusion in tissue. Dopamine plays an

important role in regulating the functions of various peripheral organs such as the heart and kidneys. The extent to which imaging of these peripheral organs with positron-labeled antisense probes is at all feasible is currently difficult to predict.

Higher Spatial Resolution

Most studies measuring dopamine receptors and dopamine transporters are done in the caudate and the putamen. However, these striatal regions are known to be functionally as well as neurochemically heterogeneous. It is anticipated that future PET instruments with higher spatial resolution and sensitivity will enable measurements in specific striatal subregions, such as the nucleus accumbens.

Integration with Functional MRI Studies

PET has benefited from advances in MRI predominantly by the use of co-registration procedures that improve regional quantitation of PET images. Also, since it is difficult to locate some brain structures in PET images due to variability in their location and size between patients, the individual subject's MRI can be used to identify them. Newer strategies are being developed for fusion imaging in which the data from both image modalities are fused to generate an image that has the spatial resolution of MRI with the biochemical information from PET. The development of functional MRI that enables assessment of functional brain activation with a higher spatial and temporal resolution than that of PET offers the opportunity of incorporating both technologies for investigating the temporal dynamics of the functional brain responses to acute changes in dopamine (i.e., temporal relationship between the receptor occupancy by an agonist and/or antagonist and its functional consequences).

Other Clinical Applications

Though D2 and DAT radioligands are being used for the evaluation of patients with movement disorders and D2 radioligands have been shown to be useful for evaluating receptor blockade by antipsychotic agents, their clinical utility has not been fully evaluated. For example, recent studies have documented a role of dopamine in malignant neuronal cell proliferation and have shown significant concentrations of D1 receptors in human brain meningiomas (*236*). Similarly, the presence of dopamine receptors, which are expressed on certain pituitary adenomas and which may be related to the cellular origins of the neoplastic cells, has been detected by the dopamine D2 receptor antagonist, ^{11}C NMS (*237*). Thus, some of the dopamine receptor radioligands may be useful in the evaluation of abnormal cell proliferation in the human brain.

CONCLUSION

PET, in conjunction with appropriate radiotracers, is being used to assess the dopamine system in the normal and the diseased human brain. As a result, information which could only be previously investigated in animals or in postmortem human brains is accessible in living human subjects. This has enabled initial investigations of the relation between changes in the dopamine system in the human brain and its functional and clinical consequences. At the same time these studies have been able to assess the effects of drugs in the dopamine system. Future advances in radiotracer development and in instrumentation will enable performance of more selective measurements with respect to the parameters investigated as well as the brain regions assessed. Such studies will increase our understanding of the mechanisms by which the dopamine system regulates motor, cognitive and motivational behaviors in the human brain.

ACKNOWLEDGMENT

This work was supported by Department of Energy grant DE-ACO2-76CH00016 and National Institute of Drug Abuse grants ROIDA06891 and ROIDA06278.

REFERENCES

1. Goldman-Rakic P. Circuitry of the prefrontal cortex. In: Plum F, ed. *Handbook of psychology.* Bethesda, MD: American Physiological Society; 1987:373–417.
2. LeMoal M, Simon H. Mesocorticolimbic dopamine network: functional and regulatory roles. *Physiol Rev* 1991;71:155–234.
3. Koob GF, Bloom FE. Cellular and molecular mechanisms of drug dependence. *Science* 1988;242:715–723.
4. Kopin IJ. The pharmacology of Parkinson's disease therapy: an update. *Ann Rev Pharmacol Toxicol* 1993;32:467–495.
5. Creese I, Burt DR, Snyder SH. Dopamine receptor binding predicts clinical and pharmacological potencies of antischizophrenic drugs. *Science* 1976;192:481–483.
6. McGeer PL, McGeer EG, Suzuki JS. Aging and extrapyramidal function. *Arch Neurol* 1977;34:33–35.
7. Weeks RA, Brooks DJ. Positron emission tomography and central neurotransmitter systems in movement disorders. *Fundam Clin Pharmacol* 1994;8:503–517.
8. Volkow ND, Fowler JS. Neuropsychiatric disorders: investigation of schizophrenia and substance abuse. *Semin Nucl Med* 1992;22:254–267.
9. Di Chiara G, Morelli M, Acquas E, Carboni E. Functions of dopamine in the extrapyramidal and limbic systems. *Arzneim-Forsch Drug Res* 1992;42:231–237.
10. Willner P, Muscat R, Papp M, Sampson D. In: Willner P, Scheel-Kruger J, eds. *The mesolimbic dopamine system: from motivation to action.* New York, NY: John Wiley and Sons; 1992:387–400.
11. Glowinski J, Tassin JP, Thierry AM. The mesocortical-prefrontal dopaminergic neurons. *TINS* 1984:418–451.
12. Selemon LD, Goldman Rackic PS. Longitudinal topography and interdigitations of corticostriatal projections in the rhesus monkey. *J Neurosci* 1984;5:776–794.
13. Stuss DT, Benson DF. *The frontal lobes.* New York, NY: Raven Press; 1986:12–38.
14. McGeer PL, Eccles JC, McGeer EG. Physiology and pharmacology of dopamine. *Molecular neurobiology of the mammalian brain.* New York, NY: Plenum Press; 1987:294–308.
15. Garris PA, Ciolkowski EL, Pastore P, Wightman RM. Efflux of dopamine from the synaptic cleft in the nucleus accumbens of the rat brain. *J Neurosci* 1994;14:6084–6093.
16. Jackson DM, Westlind-Danielsson A. Dopamine receptors: molecular biology, biochemistry and behavioral aspects. *Pharmacol Ther* 1994;64:291–369.
17. Fowler JS, Wolf AP. New directions in positron emission tomography. In: Bristol JA, ed. *Annual reports in medicinal chemistry.* 1989;24:277–286.
18. Christman DR, Hoyte RM, Wolf AP. Organic radiopharmaceuticals labeled with isotopes of short half-life. I: dopamine-hydrochloride-1-^{11}C. *J Nucl Med* 1970;11:474–478.
19. Chumpradit S, Kung MP, Billings J, Kung HF. Fluorinated and iodinated dopamine agents: D2 imaging agents for PET and SPECT. *J Med Chem* 1993;36:221–228.
20. Seeman P, Niznik H. Dopamine receptors and transporters in Parkinson's disease and schizophrenia. *FASEB J* 1990;4:2737–2744.
21. Sibley DR, Monsma FJ. Molecular biology of dopamine receptors. *Trends Pharmacol Sci* 1992;13:61–69.
22. Kessler RM, Whetsell WO, Ansari MS, et al. Identification of extrastriatal D2 receptors in postmortem human brain with [^{125}I]epidepride. *Brain Res* 1993;609:237–243.
23. Starr MS. Glutamate/dopamine D1/D2 balance in the basal ganglia and its relevance to Parkinson's disease. *Synapse* 1995;19:264–293.
24. Camps M, Cortes R, Gueye B, Probst A, Palacios JM. Dopamine receptors in human brain autoradiographic distribution of D2 sites. *Neuroscience* 1989;28:275–290.
25. Hall H, Sedvall G, Magnusson O, Kopp J, Halldin C, Farde L. Distribution of D1- and D2-dopamine receptors, and dopamine and its metabolites in human brain. *Neuropsychopharmacology* 1994;11:245–256.
26. Murray AM, Ryoo H, Joyce JN. Visualization of dopamine D3-like receptors in human brain with [^{125}I]epidepride. *Eur J Pharmacol* 1992;227:443–445.
27. Seeman P, Guan H, Van Tol H. Dopamine D4 receptors elevated in schizophrenia. *Nature* 1993;365:441–445.
28. Strange PG. Dopamine D4 receptors: curiouser and curiouser. *Trends Pharmacol Sci* 1994;15:317–319.
29. Meador-Woodruff JH, Mansour A, et al. Distribution of D5-dopamine receptor mRNA in rat brain. *Neurosc Lett* 1992;145:209–212.
30. Wagner HN, Burns HD, Dannals RF, et al. Imaging DA receptors in the human brain by PET. *Science* 1983;221:1264–1266.
31. Arnett CD, Wolf AP, Shiue CY, et al. Improved delineation of human dopamine receptors using [^{18}F]-N-methylspiroperidol and PET. *J Nucl Med* 1986;27:1878–1882.
32. Maziere B, Loc'h C, Hantraye P, et al. ^{76}Br-bromospiroperidol: a new tool for quantitative in vivo imaging of neuroleptic receptors. *Life Sci* 1984;35:1349–1356.
33. Farde L, Hall H, Ehrin E, Sedvall G. Quantitative analyses of D2-dopamine receptor binding in the living human brain by positron emission tomography. *Science* 1986;231:258–260.
34. Halldin C. Dopamine receptor radioligands. *Med Chem Res* 1994;5:127–149.
35. Seeman P, Guan C, Niznik HB. Endogenous dopamine lowers the dopamine D2 receptor density as measured by ^{3}H raclopride: implications for positron emission tomography of the human brain. *Synapse* 1989;3:96–97.
36. Wang G-J, Volkow ND, Logan J, et al. Evaluation of age-related changes in serotonin 5-HT2 and dopamine D2 receptor availability in healthy human subjects. *Life Sci* 1995;56:249–253.
37. VanTol HM, Bunzow JR, Guan C, et al. Cloning of the gene for a human dopamine D4 receptor with high affinity for the antipsychotic clozapine. *Nature* 1991;350:610–614.

38. Huntley GW, Morrison JH, Prikhozhan A, Sealton SC. Localization of multiple dopamine receptor subtype mRNAs in human and monkey motor cortex and striatum. *Mol Brain Res* 1992;15:181–188.
39. Filloux F, Dawson TM, Wamsley JK. Localization of nigrostriatal dopamine receptor subtypes and adenylate cyclase. *Brain Res Bull* 1988;20:447–459.
40. Joyce JN, Marshall JF. Quantitative autoradiography of dopamine D2 sites in rat caudate-putamen: localization to intrinsic neurons and not to neocortical afferents. *Neurosci* 1987;20:773–794.
41. Farde L, Nordstrom A-L, Karlsson P, Halldin C, Sedvall G. Positron emission tomography. Studies on dopamine receptors in schizophrenia. *Clin Neuropharmacol* 1995;18:S121–S129.
42. Wang G-J, Volkow ND, Fowler JS, et al. Comparison of two PET radioligands for imaging extrastriatal dopamine receptors in human brain. *Synapse* 1993;15:246–249.
43. Yousef K, Volkow ND, Schlyer D, et al. Inhibition of extrastriatal dopamine receptors by haloperidol. *Synapse* 1995;19:14–17.
44. Kessler RM, Whetsell WO, Ansari MS, et al. Identification of extrastriatal dopamine D2 receptors in postmortem human brain with [^{125}I]epidepride. *Brain Res* 1993;609: 237–243.
45. Halldin C, Farde L, Hogberg T, et al. Carbon-11-FLB 457: a radioligand for extrastriatal D2 dopamine receptors. *J Nucl Med* 1995;36:1275–1281.
46. Wong DF, Gjedde A, Wagner HN. Quantification of neuroreceptors in the living human brain. I. Irreversible binding of ligands. *J Cereb Blood Flow Metab* 1986;6:136–146.
47. Farde L, Halldin C, Stone-Elander S, Sedvall G. PET analysis of human dopamine receptor subtypes using ^{11}C-SCH 23390 and ^{11}C raclopride. *Psychopharmacology* 1987;92:278–284.
48. Halldin C, Farde L, Barnett A, Sedvall G. Synthesis of carbon-11-labeled SCH 39166, a new selective dopamine D1 receptor ligand, and preliminary PET investigations. *Appl Radiat Isot* 1991;42:451–455.
49. Karlsson P, Farde L, Halldin C, et al. PET examination of [^{11}C]NNC 687 and [^{11}C]NNC 756 as new radioligands for the D1-dopamine receptor. *Psychopharmacology* 1993;113:149–156.
50. Halldin C, Foged C, Loch C, et al. [^{11}C]NNC 112, a selective PET radioligand for examination of extrastriatal dopamine D1 receptors. *J Nucl Med* 1994;35:122P.
51. DaSilva JN, Wilson AA, Seeman P, Houle S. Synthesis of [^{11}C]SKF 75670 as a potential dopamine D1 receptor agonist imaging agent for PET. *J Labeled Compd Radiopharm* 1994;35:460–461.
52. Wong DF, Wagner HN Jr, Dannals RF, et al. Effects of age on dopamine and serotonin receptors measured by positron emission tomography in the living brain. *Science* 1986;226:1393–1396.
53. Baron JC, Maziere B, Loch C, et al. Loss of striatal [^{76}Br]bromospiperone binding sites demonstrated by positron emission tomography in progressive supranuclear palsy. *J Cereb Blood Flow Metab* 1986;6:131–136.
54. Antonini A, Leenders KL, Reist H, et al. Effect of age on D2 dopamine receptors in normal human brain measured by positron emission tomography and ^{11}C raclopride. *Arch Neurol* 1993;50:474–480.
55. Rinne JO, Hietala J, Ruotsalainen U, et al. Decrease in human striatal dopamine D2 receptor density with age: a PET study with ^{11}C raclopride. *J Cereb Blood Flow Metab* 1993;13:310–314.
56. Seeman P, Bzowe NH, Guan HG, et al. Human brain dopamine receptors in children and aging adults. *Synapse* 1987;1:399–404.
57. Suhara T, Fukuda H, Inoue O, et al. Age-related changes in human D1 dopamine receptors measured by positron emission tomography. *Psychopharmacology* 1991; 103:41–45.
58. Andreasen NC, Carson R, Diksic M, et al. Workshop on schizophrenia, PET and the dopamine D2 receptors in the human neostriatum. *Schiz Bull* 1988;14:471–484.
59. Farde L, Nordstrom A-L, Wiesel FA, et al. Positron emission tomography analysis of central D1 and D2 receptor occupancy in patients treated with classical neuroleptics and clozapine. Relation to extrapyramidal side effects. *Arch Gen Psychiatry* 1992; 49:538–544.
60. Smith M, Wolf AP, Brodie JD, et al. Serial ^{18}F-N-methylspiroperidol PET studies to measure changes in antipsychotic drug D2 receptor occupancy in schizophrenic patients. *Biol Psychiatry* 1988;23:653–663.
61. Farde L, Nordstrom A, Nyberg S, Halldin C, Sedvall G. D1, D2 and 5HT2 occupancy in clozapine treated patients. *J Clin Psychiatry* 1994;55(suppl B):67–69.
62. Wolkin A, Brodie JD, Rotrosen J, et al. Dopamine receptor occupancy and plasma haloperidol levels. *Arch Gen Psychiatry* 1989;46:482–483.
63. Cambon H, Baron JC, Boulenger JP. In vivo assay for neuroleptic receptor binding in the striatum positron tomography in humans. *Br J Psychiatry* 1987;151:824–830.
64. Carlsson A. Towards a new understanding of dopamine receptors. *Clin Neuropharmacol* 1995;18:S6–S13.
65. Wolkin A, Barouche F, Wolf AP, et al. Dopamine blockade and clinical response: evidence for two biological subgroups of schizophrenia. *Am J Psychiatry* 1989;46: 905–908.
66. Coppens W, Sloff CJ, Paans AMJ, et al. High central D2 dopamine receptor occupancy as assessed with positron emission tomography in medicated but therapy-resistant schizophrenic patients. *Biol Psychiatry* 1991;29:629–634.
67. Volkow ND, Fowler JS, Wolf AP, et al. Effects of chronic cocaine abuse on postsynaptic dopamine receptors. *Am J Psychiatry* 1990;147:719–724.
68. Volkow ND, Fowler JS, Wang G-J, et al. Decreased dopamine D2 receptor availability is associated with reduced frontal metabolism in cocaine abusers. *Synapse* 1993;14:169–177.
69. Hietala J, West C, Syvalahti E, et al. Striatal D2 dopamine receptor binding characteristics in vivo in patients with alcohol dependence. *Psychopharmacology* 1994;116:285–290.
70. Pearlson GD, Wong DF, Tune LE, et al. In vivo dopamine receptor density in psychotic and nonpsychotic patients with bipolar disorder. *Arch Gen Psychiatry* 1995;52:471–477.
71. Suhara T, Nakayama K, Inoue O, et al. D1 dopamine receptor binding in mood disorders measured by positron emission tomography. *Psychopharmacology* 1992; 106:14–18.
72. Caldecott-Hazzard S, Morgan DG, De Leon-Jones F, et al. Clinical and biochemical aspects of depressive disorders. II. Transmitter/receptor theories. *Synapse* 1991;9: 251–301.
73. Brown AS, Gershon S. Dopamine and depression. *J Neural Transm [Gen Sect]* 1993;91:75–109.
74. Aquilonius SM. What has PET told us about Parkinson's disease? *Acta Neurol Scand* 1991;136:37–39.
75. Rinne UK, Laihinen A, Rinne JO, et al. Positron emission tomography demonstrates dopamine D2 receptor supersensitivity in the striatum of patients with early Parkinson's disease. *Mov Disord* 1990;5:55–59.
76. Hassan MM, Thakar J. Dopamine receptors in Parkinson's disease. *Prog Neuropsychopharmacol Biol Psychiatry* 1988;12:173–182.
77. Rinne JO, Laihinen A, Lannberg P, Maramaki P, Rinne UK. A postmortem study on striatal dopamine receptors in Parkinson's disease. *Brain Res* 1991;556:117–122.
78. Schwartz J, Tatsch K, Arnold G, et al. ^{123}I-iodobenzamide-SPECT predicts dopaminergic responsiveness in patients with de novo parkinsonism. *Neurology* 1992;41: 556–561.
79. Leenders K, Frackowiak R, Quinn N. Brain energy metabolism and dopaminergic functions in Huntington's disease measured in vivo using positron emission tomography. *Mov Disord* 1986;1:69–77.
80. Hagglund J, Aquilonius S-M, Eckernas S-A, et al. Dopamine receptor properties in Parkinson's disease and Huntington's chorea evaluated by positron emission tomography using ^{11}C-N-methylspiperone. *Acta Neurol Scand* 1987;75:87–94.
81. Brandt J, Folstein S, Wong D, et al. D2 receptors in Huntington's disease: positron emission tomography findings and clinical correlates. *J Neuropsychiatry Clin Neurosci* 1990;2:20–27.
82. Sedvall G, Karlsson P, Lundin A, et al. Dopamine D1 receptor number—a sensitive PET marker for early brain degeneration in Huntington's disease. *Eur Arch Psychiatry Clin Neurosci* 1994;243:249–255.
83. Ritz MC, Lamb RJ, Goldberg SR, Kuhar MJ. Cocaine receptors on dopamine transporters are related to self administration of cocaine. *Science* 1987;237:1219–1223.
84. Salmon E, Brooks DJ, Leenders KL, et al. A two-compartment description and kinetic procedure for measuring [^{11}C]nomifensine uptake using positron emission tomography. *J Cereb Blood Flow Metab* 1990;10:307–317.
85. Tedroff J, Aquilonius S-M, Hartvig P, et al. Monoamine reuptake sites in the human brain evaluated in vivo by means of ^{11}C nomifensine and positron emission tomography: the effect of age and Parkinson's disease. *Acta Neurol Scand* 1988;77: 92–101.
86. Fowler JS, Volkow ND, Wolf AP, et al. Mapping cocaine binding sites in human and baboon brain in vivo. *Synapse* 1989;4:371–377.
87. Kilbourn MR. In vivo binding of [^{18}F]GBR 13119 to the brain dopamine uptake system. *Life Sci* 1988;42:1347–1351.
88. Kilbourn MR, Haka MS, Mulholland GK, Jewett DM, Kuhl D. Synthesis of radiolabeled inhibitors of presynaptic monoamine uptake systems: [^{18}F]GBR 13119 (DA), [^{11}C]nisoxetine (NE) and [^{11}C]fluoxetine (5-HT). *J Lab Cmpd Radiopharm* 1989;26:412–414.
89. Koeppe RA, Kilbourn MR, Frey KA, et al. Imaging and kinetic modeling of [^{18}F]GBR 12909, a dopamine uptake inhibitor. *J Nucl Med* 1990;31:720.
90. Innis RB, Seibyl JP, Scanley BE, et al. Single-photon emission computed tomographic imaging demonstrates loss of striatal dopamine transporters in Parkinson's disease. *Proc Natl Acad Sci USA* 1993;90:11965–11969.
91. Laihinen AO, Rinne JO, Nagren KA, et al. PET studies on brain monoamine transporters with carbon-11-β-CIT in Parkinson's disease. *J Nucl Med* 1995;36: 1263–1267.
92. Madras BK, Spealman RD, Fahey MA, et al. Cocaine receptors labeled by 2β-carbomethoxy-3β-(4-fluorophenyl)tropane. *Mol Pharm* 1989;36:518–524.
93. Wong DF, Yung B, Dannals RF, et al. In vivo imaging of baboon and human dopamine transporters by positron emission tomography using [^{11}C]WIN 35,428. *Synapse* 1993;15:130–142.
94. Frost JJ, Rosier AJ, Reich SG, et al. Positron emission tomographic imaging of the dopamine transporter with ^{11}C-WIN 35,428 reveals marked declines in mild Parkinson's disease. *Am J Neurol* 1993;34:423–431.
95. Ding Y-S, Fowler JS, Volkow ND, et al. Pharmacokinetics and in vivo specificity of [^{11}C]d-threo-methylphenidate for the presynaptic dopaminergic neuron. *Synapse* 1994;18:152–160.
96. Volkow ND, Ding YS, Fowler JS, et al. [^{11}C]d-threo-methylphenidate: a new PET ligand for the dopamine transporter. II. Studies in the human brain. *J Nucl Med* 1995;36:2162–2168.
97. Aquilonius S-M, Bergstrom K, Eckernas SA, et al. In vivo evaluation of striatal dopamine reuptake sites using ^{11}C-nomifensine and positron emission tomography. *Acta Neurol Scand* 1987;76:283–287.
98. Volkow ND, Fowler JS, Logan J, et al. Comparison of [^{11}C]cocaine binding at sub-pharmacological and pharmacological doses: a PET study. *J Nucl Med* 1995;36: 1289–1297.
99. Kilbourn MR, DaSilva JN, Frey KA, Koeppe RA, Kuhl DE. In vivo imaging of vesicular monoamine transporters in human brain using [^{11}C]tetrabenazine and positron emission tomography. *J Neurochem* 1993;60:2315–2318.
100. Kilbourn MR. Shades of grey: radiopharmaceutical chemistry in the 1990s and beyond. *Nucl Med Biol* 1992;19:603–606.
101. Volkow ND, Fowler JS, Wang G-J, et al. Decreased dopamine transporters with age in healthy human subjects. *Ann Neurology* 1994;36:237–239.
102. Van Dick CH, Seibyl JP, Malison RT, et al. Age-related decline in dopamine transporter binding in human striatum with [I-123]β-CIT SPECT. *J Nucl Med* 1995;36:1175–1181.
103. Zelnik N, Angel I, Paul SM, Kleinman JE. Decreased density of human striatal dopamine uptake sites with age. *Eur J Pharmacol* 1986;126:175–176.

104. De Keyser J, Ebinger G, Vauquelin G. Age-related changes in the human nigrostriatal dopaminergic system. *Ann Neurol* 1990;27:157–161.
105. Malison RT, Wallace EA, Best S, et al. SPECT imaging of dopamine transporters in cocaine dependent and healthy control subjects with [^{123}I]βCIT. *Soc Neurosci Abstr* 1994;20:1625.
106. Volkow ND, Wang G-J, Fowler JS, et al. Cocaine binding is decreased in the brain of detoxified cocaine abusers. *J Neuropsychopharmacol* 1996;14:159–168.
107. Tiihonen J, Kuikka J, Bergstrom K, et al. Altered striatal dopamine reuptake site densities in habitually violent and nonviolent alcoholics. *Nature Medicine* 1995;1: 654–657.
108. Zhu M-Y, Juorio AV. Aromatic L-amino acid decarboxylase: biological characterization and functional role. *Gen Pharmacol* 1995;26:681–696.
109. Cumming P, Venkatachalam TK, Rajagopal S, Diksic M, Gjedde A. Brain uptake of α-[^{14}C]methyl-para-tyrosine in the rat. *Synapse* 1994;17:125–128.
110. DeJesus OJ, Murali D, Kitchen R, et al. Evaluation of 3[^{18}F]fluoro-α-fluoromethyl-p-tyrosine, a potential PET tracer for tyrosine hydroxylase activity. *Nucl Med Biol* 1994;21:663–667.
111. Garnett ES, Firnau G, Nahmias C. Dopamine visualized in the basal ganglia of living man. *Nature* 1983;305:137–138.
112. Garnett ES, Firnau G, Chan PKH, Sood S, Belbeck LW. [^{18}F]Fluoro-dopa, an analog of dopa, and its use in direct external measurements of storage, degradation and turnover of intracerebral dopamine. *Proc Nat Acad Sci USA* 1978;75:464–467.
113. Hoshi H, Kuwabara H, Leger G, Cumming P, Guttman M, Gjedde A. 6-[^{18}F]Fluoro-L-dopa metabolism in living human brain: a comparison of six analytical methods. *J Cereb Blood Flow Metab* 1993;13:57–69.
114. Dhawan V, Ishikawa T, Chaley T, et al. Combined FDOPA and 3OMFD PET studies in Parkinson's disease: modeling issues. *J Nucl Med* 1996;in press.
115. Melega WP, Hoffman JM, Luxen A, et al. The effects of carbidopa on the metabolism of 6-[^{18}F]fluoro-L-dopa in rats, monkeys and humans. *Life Sci* 1990;47:149–157.
116. Gjedde A, Reith J, Dyve S, et al. Dopa decarboxylase activity in the living human brain. *Proc Nat Acad Sci USA* 1991;88:2721–2725.
117. Hartvig P, Lindner KJ, Tedroff J, et al. Regional brain kinetics of 6-fluoro-(β-^{11}C)-L-dopa and (β-^{11}C)-L-dopa following COMT inhibition. A study in vivo using positron emission tomography. *J Neural Transm* 1992;87:15–22.
118. Melega WP, Luxen A, Perlmutter MM, et al. Comparative in vivo metabolism of 6-[^{18}F]fluoro-L-dopa and [^{3}H]L-dopa in rats. *Biochem Pharm* 1990;39:1853–1860.
119. Hartvig P, Agren H, Reibring L, et al. Brain kinetics of L-[β-^{11}C]DOPA in humans studied by positron emission tomography. *J Neural Transm* 1991;86:25–41.
120. Agren H, Reibring L, Hartvig P, et al. Monoamine metabolism in human prefrontal cortex and basal ganglia. PET studies using [β-^{11}C]L-5-hydroxytryptophan and [β-^{11}C]L-DOPA in healthy volunteers and patients with unipolar depression. *Depression* 1993;1:71–81.
121. Snow BJ, Tooyama I, McGeer EG, et al. Human positron emission tomographic [^{18}F]fluorodopa studies correlate with dopamine cell counts and levels. *Ann Neurol* 1993;34:324–330.
122. Eidelberg D, Takikawa S, Dhawan V, et al. Striatal ^{18}F-DOPA uptake: absence of an aging effect. *J Cereb Blood Flow Metab* 1993;13:881–888.
123. Martin WRW, Palmer MR, Patlak CS, Calne DB. Nigro-striatal function in man studied with positron emission tomography. *Ann Neurol* 1989;26:535–542.
124. Sawle GV, Colebatch JG, Shah A, et al. Striatal function in normal aging: implications for Parkinson's disease. *Ann Neurol* 1990;28:799–804.
125. Kish SJ, Zhong XH, Hornykiewicz O, et al. Striatal 3,4-dihydroxyphenylalanine decarboxylase in aging: disparity between postmortem and positron emission tomography studies. *Ann Neurol* 1995;38:260–264.
126. Holthoff VA, Kessler J, Pietrzyk U, et al. Motor and cognitive deficits in Parkinson's disease are related to striatal dopamine uptake [Abstract]. *J Cereb Blood Flow Metab* 1993;13:S253.
127. DeJesus OT, Mukhergee J. Radiobrominated m-tyrosine analogs as potential CNS L-dopa PET tracers. *Biochem Biophys Res Commun* 1988;150:1027–1031.
128. Melega WP, Perlmutter MM, Luxen A, et al. 4-[^{18}F]Fluoro-L-m-tyrosine: An L-3,4-dihydroxyphenylalanine analog for probing presynaptic dopaminergic function with positron emission tomography. *J Neurochem* 1989;53:311–314.
129. Nahmias C, Wahl L, Chirakal R, et al. A probe for intracerebral aromatic amino-acid decarboxylase activity: distribution and kinetics of [^{18}F]6-fluoro-L-m-tyrosine in the human brain. *Mov Disord* 1995;10:298–304.
130. DeJesus OT, Holden JE, Endres C, et al. Visualization of dopamine nerve terminals by positron tomography using [^{18}F]fluoro-β-fluoromethylene-m-tyrosine. *Brain Res* 1992;597:151–154.
131. Berry MD, Juorio AV, Paterson IA. The functional role of monoamine oxidases A and B in the mammalian central nervous system. *Prog Neurobiol* 1994;42:375–391.
132. Breakefield XO, Chen Z-Y, Tivol E, Shalish C. Molecular genetics and inheritance of human monoamine oxidases A and B. *Neurol Dis Ther* 1994;21:95–112.
133. Youdim MBH, Riederer P. Dopamine metabolism and neurotransmission in primate brain in relationship to monoamine oxidase A and B inhibition. *J Neural Transm* 1993;91:181–195.
134. O'Carroll M, Fowler CJ, Phillips JP, et al. The deamination of dopamine by human brain monoamine oxidase. Specificity for the two enzyme forms in seven brain regions. *Arch Pharmacol* 1983;322:198–202.
135. Johnston JP. Some observations upon a new inhibitor of monoamine oxidase in brain tissue. *Biochem Pharmacol* 1968;17:1285–1297.
136. Knoll J, Magyar K. Some puzzling effects of monoamine oxidase inhibitors. *Adv Biochem Psychopharmacol* 1972;5:393–408.
137. Oreland L, Arai Y, Stenstrom A, Fowler CJ. Monoamine oxidase activity and localization in the brain and the activity in relation to psychiatric disorders. *Mod Prob Pharmacopsychiatry* 1983;19:246–254.
138. Riederer P, Konradi C, Schay V, et al. Localization of MAO A and MAO B in human brain: a step in understanding the therapeutic action of L-deprenyl. In: Yahr MD, Bergman KJ, eds. *Advances in Neurology*. New York, NY: Raven Press, 1986:111–118.
139. Strolin, Benedetti M, Dostert P. Monoamine oxidase: from physiology and pathophysiology to the design and clinical application of reversible inhibitors. *Adv Drug Research* 1992;23:67–125.
140. Birkmayer W, Knoll J, Youdim MBH, et al. Increased life expectancy resulting from addition of L-deprenyl to L-DOPA treatment in Parkinson's disease: a longterm study. *J Neural Transm* 1985;64:113–127.
141. Tetrud JW, Langston JW. The effect of deprenyl (selegeline) on the natural history of Parkinson's disease. *Science* 1989;245:519–522.
142. Olanow CW, Calne D. Does selegeline monotherapy in Parkinson's disease act by symptomatic or protective mechanisms? *Neurology* 1991;41 (suppl 4):13–26.
143. Fowler JS, MacGregor RR, Wolf AP, et al. Mapping human brain monoamine oxidase A and B with ^{11}C-suicide inactivators and positron emission tomography. *Science* 1987;235:481–485.
144. Shinotoh H, Inoue O, Suzuki K, et al. Kinetics of [^{11}C]N,N-dimethylphenethylamine in mice and humans: potential for measurement of brain MAO B activity. *J Nucl Med* 1987;28:1006–1011.
145. Fowler JS, Wang G-J, Logan J, et al. Selective reduction of radiotracer trapping by deuterium substitution: comparison of [^{11}C]L-deprenyl and [^{11}C]L-deprenyl-D2 for MAO B mapping. *J Nucl Med* 1995;36:1255–1262.
146. Fowler JS, Volkow ND, Logan J, et al. Slow recovery of human brain MAO B after L-Deprenyl (selegeline) withdrawal. *Synapse* 1994;18:86–93.
147. Bench CJ, Price GW, Lammertsma AA, et al. Measurement of human cerebral monoamine oxidase B (MAO B) activity with positron emission tomography (PET): a dose ranging study with the reversible inhibitor Ro 19 6327. *Eur J Clin Pharmacol* 1991;10:169–173.
148. Fowler JS, Volkow ND, Logan J, et al. MAO B inhibition therapy in Parkinson's disease: the degree and reversibility of human brain MAO B inhibition by RO 196327. *Neurology* 1993;42:1984–1992.
149. Guldberg HC, Marsden CA. Catechol-O-methyltransferase: pharmacological aspects and physiological role. *Pharmacol Rev* 1975;27:135–206.
150. Mannisto TP, Kaakkola S. New selective COMT inhibitors: useful adjuncts for Parkinson's disease? *TIPS* 1989;10:34–36.
151. Wood PL, Altar CA. Dopamine release in vivo from nigrostriatal mesolimbic and mesocortical neurons: utility of 3-methoxytyramine measurements. *Pharmacol Rev* 1988;40:163–187.
152. Axelrod J. The O-methylation of epinephrine and other catechols in vitro and in vivo. *Science* 1957;126:1657–1660.
153. Mannisto PT, Kaakkola S, Nissinen E, et al. Potent, selective and orally active inhibitors of catechol-O-methyltransferase. *Life Sci* 1988;32:1465–1471.
154. Ding YS, Gatley SJ, Fowler JS, et al. Mapping catechol-O-methyltransferase (in vivo—initial studies with [^{18}F] Ro41-0960. *Life Sci* 1995;58:195–208.
155. Friedman AM, DeJesus OJ, Revenaugh J, et al. Measurements in vivo of parameters of the dopamine system. *Ann Neurol* 1984;15:S66–S76.
156. Ross SB, Jackson DM. Kinetic properties of the accumulation of ^{3}H raclopride in the mouse in vivo. *Arch Pharmacol* 1989;340:6–12.
157. Dewey SL, Smith GW, Logan J, et al. GABAergic inhibition of endogeneous dopamine release measured in vivo with ^{11}C-raclopride and positron emission tomography. *J Neurosci* 1992;12:3773–3780.
158. Dewey SL, Smith GS, Logan J, et al. Striatal binding of the PET ligand ^{11}C-raclopride is altered by drugs that modify synaptic dopamine levels. *Synapse* 1993;13:350–356.
159. Hume SP, Myers R, Bloomfield PM, et al. Quantitation of carbon-11-labeled raclopride in rat striatum using positron emission tomography. *Synapse* 1992;12:47–54.
160. Volkow ND, Wang G-J, Fowler JS, et al. Imaging endogenous dopamine competition with [^{11}C]raclopride in the human brain. *Synapse* 1994;16:255–262.
161. Dewey SL, Logan J, Wolf AP, et al. Amphetamine induced decreases in [^{18}F] N-methylspiroperidol binding in baboon brain using positron emission tomography (PET). *Synapse* 1991;7:324–327.
162. Logan J, Dewey SL, Wolf AP, et al. Effects of endogenous dopamine on measures of [^{18}F]N-methylspiroperidol binding in the basal ganglia: comparison of simulations and experimental results from PET studies in baboons. *Synapse* 1991;9:195–207.
163. Nordstrom AL, Farde L, Pauli S, et al. PET analysis of central [^{11}C]raclopride binding in healthy young adults and schizophrenic patients, reliability and age effects. *Human Psychopharmacol* 1992;7:157–165.
164. Volkow ND, Fowler JS, Wang G-J, et al. Reproducibility of repeated measures of ^{11}C raclopride binding in the human brain. *J Nucl Med* 1993;34:609–613.
165. Laruelle M, Abi-Dargham A, van Dick C, et al. SPECT imaging of striatal dopamine release after amphetamine challenge. *J Nucl Med* 1995;36:1182–1190.
166. Wang G-J, Volkow ND, Fowler JS, et al. Methylphenidate decreases regional cerebral blood flow in normal human subjects. *Life Sci* 1994;54:1433–1446.
167. Logan J, Volkow ND, Fowler JS, et al. Effects of blood flow on [^{11}C] raclopride binding in the brain: model simulations and kinetic analysis of PET data. *J Cereb Blood Flow Metab* 1994;14:995–1010.
168. Inoue O, Tsukada H, Kobayashi K, et al. Swim stress alters in vivo binding of [^{3}H]N-methylspiperone. *Neuropharmacol* 1991;30:1101–1106.
169. Deterding LJ, Dix K, Burka LT, Tomer KB. On-line coupling of in vivo microdialysis with tandem mass spectrometry. *Anal Chem* 1992;64:2636–2641.
170. Gifford AN, Gatley SJ, Ashby CR. Endogeneously released dopamine inhibits the binding of dopaminergic PET and SPECT ligands in superfused rat striatal slices. *Synapse* 1990;22:232–238.
171. Riederer P, Lange KW, Kornhuber J, et al. Glutamatergic-dopaminergic balance in the brain: its implications in motor disorders and schizophrenia. *Arzneim-Forsch* 1992;42:265–268.
172. Meltzer H. Clinical studies on the mechanism of action of clozapine: the dopamine-serotonin hypothesis of schizophrenia. *Psychopharmacol* 1989;99:S18–S27.
173. Schaefer GJ. Opiate antagonists and rewarding brain stimulation. *Neurosci Behav Rev* 1988;12:1–17.
174. Girault JA, Halpain S, Greengard P. Excitatory amino acid antagonists and Parkinson's disease. *Trends Neurosci* 1990;13:325–326.

175. Stockmeier CA, DiCarlo JJ, Zhang Y, et al. Characterization of typical and atypical antipsychotic drugs based on in vivo occupancy of serotonin-2 and dopamine-2 receptors. *J Pharmacol Exp Ther* 1993;266:1374–1384.
176. Dewey SL, Brodie JD, Fowler JS, et al. Positron emission tomography studies of dopaminergic/cholinergic interactions in the baboon brain. *Synapse* 1990;6:321–327.
177. Dewey SL, Smith GS, Logan J, et al. Effects of central cholinergic blockade on striatal dopamine release measured with positron emission tomography in normal human subjects. *Proc Natl Acad Sci USA* 1993;90:11816–11820.
178. Dewey SL, Smith GS, Logan J, et al. Serotonergic modulation of striatal dopamine measured with positron emission tomography and in vivo microdialysis. *J Neurosci* 1995;15:821–829.
179. Smith GS, Dewey SL, Logan J, et al. Opiate modulation of striatal dopamine release measured with positron emission tomography and ^{11}C-raclopride [Abstract]. *Soc Neurosci Abstr* 1993;19:128.9.
180. Ingvar M, Stone-Elander S, Rogers G, et al. Striatal D2/acetylcholine interactions: PET studies of the vesamicol receptor. *NeuroReport* 1993;4:1311–1314.
181. Reith J, Benkelfat C, Sherwin A, et al. Elevated dopa decarboxylase activity in living brain of patients with psychosis. *Proc Natl Acad Sci USA* 1994;91:11651–11654.
182. Grace AA. Phasic versus tonic dopamine release and the modulation of the dopamine system responsivity. *Neurosci* 1991;41:1–24.
183. Reivich M, Kuhl D, Wolf AP, et al. The [^{18}F]fluorodeoxyglucose method for the measurement of local cerebral glucose utilization in man. *Circ Res* 1979;44:127–137.
184. Mata M, Fink DJ, Gainer H. Activity-dependent energy metabolism in rat posterior pituitary primarily reflects sodium pump activity. *J Neurochem* 1980;34:213–215.
185. Sokoloff L, Reivich M, Kennedy C, et al. The [^{14}C]deoxyglucose method for measurement of local cerebral glucose utilization. *J Neurochem* 1977;28:897–916.
186. Porrino LJ, Crane AM. Metabolic mapping of the effects of drugs of abuse with the 2-[^{14}C]deoxyglucose method. *Modern methods in pharmacology, volume 6, testing and evaluation of drugs of abuse.* New York, NY: Wiley-Liss; 1990:147–164.
187. Wolkin A, Angrist B, Wolf A, et al. Effects of amphetamine on local cerebral metabolism in normal and schizophrenic subjects as determined by positron emission tomography. *Psychopharmacol* 1987;92:241–246.
188. London ED, Cascella NG, Wong DF, et al. Cocaine-induced reduction of glucose utilization in human brain. A study using positron emission tomography and [fluorine-18]-fluorodeoxyglucose. *Arch General Psychiatry* 1990;47:567–574.
189. Volkow ND, Brodie JD, Wolf AP, et al. Brain metabolism in schizophrenics before and after acute neuroleptic administration. *J Neurol Neurosurg Psychiatry* 1986;49: 1199–1202.
190. Bartlett EJ, Brodie JD, Simkowitz P, et al. Effects of haloperidol challenge on regional cerebral glucose utilization in normal human subjects. *Am J Psychiatry* 1994;151:681–686.
191. Wolkin A, Jaeger J, Brodie JD, et al. Persistence of cerebral metabolic abnormalities in chronic schizophrenia as determined by positron emission tomography. *Am J Psychiatry* 1985;142:564–571.
192. DeLisi LE, Holcomb HH, Cohen RM, et al. Positron emission tomography in schizophrenic patients with and without neuroleptic medication. *J Cereb Blood Flow Metab* 1985;5:201–206.
193. Buchsbaum MS, Wu JC, DeLisi LE, et al. Positron emission tomography studies of basal ganglia and somatosensory cortex neuroleptic drug effects. *Biol Psychiatry* 1987;22:479–494.
194. Szechtman H, Nahmias C, Garnett ES, et al. Effect of neuroleptics on altered cerebral glucose metabolism in schizophrenia. *Arch Gen Psychiatry* 1988;45:523–532.
195. Wik G, Wiesel F-A, Sjorgen I, et al. Effects of sulpiride and chlorpromazine on regional cerebral glucose metabolism in schizophrenic patients as determined by positron emission tomography. *Psychopharmacol* 1989;97:309–318.
196. Buchsbaum MS, Potkin SG, Siegel BV Jr, et al. Striatal metabolic rate and clinical response to neuroleptics in schizophrenia. *Arch Gen Psychiatry* 1992;49:966–974.
197. Bartlett EJ, Wolkin A, Brodie JD, et al. Importance of pharmacologic control in PET studies: effects of thiothixene and haloperidol on cerebral glucose utilization in chronic schizophrenia. *Psychiatry Res* 1991;40:115–124.
198. Holcomb HH, Cascella NG, Thaker GK, et al. Functional sites of neuroleptic drug action in the human brain: PET/FDG studies with and without haloperidol. *Am J Psychiatry* 1996;153:41–49.
199. Eidelberg D, Moeller JR, Ishikawa T, et al. Early differential diagnosis of Parkinson's disease with ^{18}F-fluorodeoxyglucose and positron emission tomography. *Neurology* 1995;45:1995–2004.
200. Eidelberg D, Moeller JR, Dhawan V, et al. The metabolic anatomy of Parkinson's disease: complementary ^{18}F-fluorodeoxyglucose and ^{18}F-fluorodopa positron emission tomography studies. *Mov Disord* 1990;5:203–213.
201. Swart JAA, Korf J. In vivo dopamine receptor assessment for clinical studies using positron emission tomography. *Biochem Pharmacol* 1987;36:2241–2250.
202. Mintun MA, Raichle ME, Kilbourn MR, et al. A quantitative model for the in vivo assessment of drug binding sites with positron emission tomography. *Ann Neurol* 1984;15:217–227.
203. Wong DF, Gjedde A, Wagner HN, et al. Quantification of neuroreceptors in the living human brain. II. Inhibition studies of receptor density and affinity. *J Cereb Blood Flow Metab* 1986;6:147–153.
204. Farde L, Eriksson L, Blomquist G, Halldin C. Kinetic analysis of central [^{11}C]raclopride binding to D2-dopamine receptors studied by PET—a comparison to the equilibrium analysis. *J Cereb Blood Flow Metab* 1989;9:696–708.
205. Perlmutter JS, Larson KB, Raichle ME, et al. Strategies for in vivo measurement of receptor binding using positron emission tomography. *J Cereb Blood Flow Metab* 1986;6:154–169.
206. Logan J, Wolf AP, Shiue C-Y, Fowler JS. Kinetic modeling of a receptor-ligand binding applied to positron emission tomographic studies with neuroleptic tracers. *J Neurochem* 1987;48:73–83.
207. Patlak CS, Blasberg RG, Fenstermacher JD. Graphical evaluation of blood-to-brain transfer constants from multiple-time uptake data. *J Cereb Blood Flow Metab* 1983;3:1–7.
208. Patlak CS, Blasberg RG. Graphical evaluation of blood-to-brain transfer constants from multiple-time uptake data. Generalization. *J Cereb Blood Flow Metab* 1985;5: 584–590.
209. Logan J, Fowler JS, Volkow ND, et al. Graphical analysis of reversible radioligand binding from time-activity measurements applied to [N-^{11}C-methyl]-(−)-cocaine PET studies in human subjects. *J Cereb Blood Flow Metab* 1990;10:740–747.
210. Koeppe RA, Holthoff VA, Frey KA, et al. Compartmental analysis of [^{11}C]flumazenil kinetics for the estimation of ligand transport rate and receptor distribution using positron emission tomography. *J Cereb Blood Flow Metab* 1991;11:735–744.
211. Carson RE. Parameter estimation in positron emission tomography. In: Phelps M, Mazziotta J, Schelbert H, eds. *Positron emission tomography and autoradiography: principles and applications for the brain and heart.* New York, NY: Raven Press; 1986:347–390.
212. Huang S-C, Barrio JR, Phelps ME. Neuroreceptor assay with positron emission tomography: equilibrium versus dynamic approaches. *J Cereb Blood Flow Metab* 1986;6:515–521.
213. Zeeberg BR, Gibson RE, Reba RC. Accuracy of in vivo neuroreceptor quantification by PET and review of steady-state, transient, double injection and equilibrium models. *IEEE Trans Med Imaging* 1988;7:203–215.
214. Delforge J, Syrota A, Mazoyer BM. Experimental design optimization: theory and application to estimation of receptor model parameters using dynamic positron emission tomography. *Phys Med Biol* 1989;34(4):419–435.
215. Logan J, Schlyer DJ, Wolf AP, et al. Antipsychotics D-2 receptor occupancy and plasma concentration. *Biol Psychiatry* (Letter) 1990;28:1068–1070.
216. Holthoff VA, Koeppe RA, Frey KA, et al. Differentiation of radioligand delivery and binding in the brain: validation of a two-compartment model for [^{11}C]flumazenil. *J Cereb Blood Flow Metab* 1991;11:745–752.
217. Carson RE, Channing MA, Blasberg RG, et al. Comparison of bolus and infusion methods for receptor quantitation: application to [^{18}F]cyclofoxy and positron emission tomography. *J Cereb Blood Flow Metab* 1993;13:24–42.
218. Wong DF, Wagner HN Jr, Tune LE, et al. Positron emission tomography reveals elevated D2-dopamine receptors in drug-naive schizophrenics. *Science* 1986;234: 1558–1563.
219. Farde L, Wiesel F-A, Stone-Elander S, et al. D2-dopamine receptors in neuroleptic-naive schizophrenic patients. *Arch Gen Psychiatry* 1990;47:213–219.
220. Votaw JR, Kessler RM, De Paulis T. Failure of the three-compartment model to describe the pharmacokinetics in brain of a high affinity substituted benzamide. *Synapse* 1993;15:177–190.
221. Samana P, Cottechia S, Costa T, Lefkowitz RJ. A mutation-induced activated state of the β2-adrenergic receptor. *J Biol Chem* 1993;268:4625–4636.
222. Costa T, Ogino Y, Munson PJ, et al. Drug efficacy at guanine nucleotide-binding regulatory protein-linked receptors: thermodynamic interpretation of negative antagonism and of receptor activity in the absence of ligand. *Mol Pharmacol* 1992;41: 549–560.
223. Black JW, Shankley NP. Inverse agonists exposed. *Nature* 1995;374:214–215.
224. Bond RA, Leff P, Johnson TD, et al. Physiological effects of inverse agonists in transgenic mice with myocardial overexpression of the β2-adrenoceptor. *Nature* 1995;374:272–276.
225. Leff P. The two-state model of receptor activation. *Trends Pharmacol Sci* 1994;15: 408–409.
226. Milligan G, Bond RA, Lee M. Inverse agonists: pharmacological curiosity or potential therapeutic strategy? *Trends Pharmacol Sci* 1995;16:10–13.
227. Tiberi M, Caron MC. Constitutive activity of dopamine D1 receptor subtypes. *Clin Neuropharmacol* 1995;18:S43–S48.
228. Robinson PR, Cohen GB, Zhukovsky EA, Oprian DD. Constitutively active mutants of rhodopsin. *Neuron* 1992;9:719–725.
229. Parma J, Duprez L, Van Sande J, et al. Somatic mutations in the thyrotropin receptor gene cause hyperfunctioning thyroid adenomas. *Nature* 1993;365:649–651.
230. Yang Z-Y, Mukherjee J. Development of agonists as radiotracers for the assessment of the functional state of the dopamine D2 receptors [Abstract]. *J Nucl Med* 1995;36(suppl):152P.
231. Manji HK, Chen G, Simon H, et al. Guanine nucleotide-binding proteins in bipolar affective disorder. *Arch Gen Psychiatry* 1995;52:135–144.
232. Nestler EJ. Molecular neurobiology of drug addiction. *Neuropsychopharmacol* 1994;11:77–88.
233. Manji HK, Potter WZ, Lenox RH. Signal transduction pathways. Molecular targets for lithium's actions. *Arch Gen Psychiatry* 1995;52:531–543.
234. Takahashi T, Ido T, Ootake A, et al. [^{18}F]Labeled 1,2-diacylglycerols; a new tracer for the imaging of second messenger system [Abstract]. *J Labeled Compds Radiopharm* 1994;35:517–519.
235. Dewanjee MK, Ghafouripour AK, Boothe T, et al. Gallium-67 labeling of antisense deoxyoligonucleotide (GAASDON) probes and uptake in leukemic cells (P388) [Abstract]. *J Labeled Compd Radiopharm* 1994;35:356–357.
236. Schrell UM, Nomikos P, Fahlbusch R. Presence of dopamine D1 receptors and absence of dopamine D2 receptors in human cerebral meningioma tissue. *J Neurosurg* 1992;77:288–294.
237. Muhr C, Bergstrom M, Lundberg PO, et al. Dopamine receptors in pituitary adenomas: PET visualization with ^{11}C-N-methylspiperone. *J Comp Assist Tomog* 1986;10:175–180.
238. Luabeya MK, Maloteaux JM, Laduron PM. Regional and cortical laminar distributions of serotonin S2, benzodiazepine, muscarinic and dopamine D2 receptors in human brain. *J Neurochem* 1984;43:1068–1071.
239. McElvain JS, Schenk JO. A multisubstrate mechanism of striatal dopamine uptake and its inhibition by cocaine. *Biochem Pharmacol* 1992;43:2189–2199.
240. Mackay AVP, Davies P, Dewar CM, Yates CM. Regional distribution of enzymes associated with neurotransmission by monoamines, acetylcholine and GABA in the human brain. *J Neurochem* 1978;30:827–839.
241. O'Carroll AM, Anderson MC, Tobbia I, et al. Determination of the absolute concentrations of monoamine oxidase A and B in human tissues. *Biochem Pharmacol* 1989;38:901–905.

242. Huh MM, Friedhoff AJ. Multiple molecular forms of catechol-O-methyltransferase. *J Biol Chem* 1979;254:299–308.
243. Kastner A, Anglade P, Bounaix C, et al. Immunohistochemical study of catechol-O-methyltransferase in the human mesostriatal system. *Neurosci* 1994;62:449–457.
244. Andersen PH, Gronvald FC, Hohlweg R, et al. NNC-112, NNC-687 and NNC-756: new, selective and highly potent dopamine D1-receptor antagonists. *Eur J Pharmacol* 1992;219:45–52.
245. Inoue O, Kobayashi K, Sakiyama Y, Suzuki T. The effect of benzodiazepines on the binding of [^{3}H]SCH 23390 in vivo. *Neuropharmacol* 1992;31:115–121.
246. Farde L, Ehrin E, Eriksson L, et al. Substituted benzamides as ligands for visualization of dopamine receptor binding in the human brain by positron emission tomography. *Proc Natl Acad Sci USA* 1985;82:3863–3867.
247. Inoue O, Kobayashi K, Tsukada H, et al. Differences in in vivo receptor binding between [^{3}H]N-methylspiperone and [^{3}H]raclopride in reserpine-treated mouse brain. *J Neural Transm* 1991;85:1–10.
248. Kung HF, Pan S, Kung MP, et al. In vitro and in vivo evaluation of [^{123}I]IBZM: a potential CNS D2-dopamine receptor imaging agent. *J Nucl Med* 1989;30:88–92.
249. Kessler RM, Ansari MS, Schmidt DE, et al. High-affinity dopamine D2 receptor radioligands. 2. [^{123}I]epidepride, a potent and specific radioligand for the characterization of striatal and extrastriatal dopamine D2 receptors. *Life Sci* 1991;49:617–628.
250. Pellevoisin C, Chalon S, Zouakia A, et al. Comparison of two radioiodinated ligands of dopamine D2 receptors in animal models: iodobenzamide and iodoethylspiperone. *Life Sci* 1993;52:1851–1860.
251. Laruelle M, Wallace E, Seibyl JP, et al. Graphical, kinetic and equilibrium analyses of in vivo [^{123}I]β-CIT binding to dopamine transporters in healthy human subjects. *J Cereb Blood Flow Metab* 1994;14:982–994.
252. Gatley SJ, Ding Y-S, Volkow ND, et al. Binding of d-threo-[^{11}C]methylphenidate to the dopamine transporter in vivo: insensitivity to synaptic dopamine. *Eur J Pharmacol* 1995;281:141–149.
253. Volkow ND, Fowler JS, Wolf AP, et al. Distribution and kinetics of carbon-11-cocaine in the human body measured with PET. *J Nucl Med* 1992;33:521–525.
254. Scheffel U, Boja JW, Kuhar MJ. Cocaine receptors: in vivo labeling with ^{3}H-(−)cocaine, ^{3}H-WIN 35,065-2 and ^{3}H-WIN 35,428. *Synapse* 1989;4:390–392.

Ethical Clinical Practice of Functional Brain Imaging

Society of Nuclear Medicine Brain Imaging Council
Reston, Virginia

The development and evolution of functional brain imaging technologies and their broad application to a wide range of neurological and psychiatric disorders have led to their scientifically sound use in specific clinical situations. In addition, there is a growing diversity of empirical new applications where there is little previous research or clinical experience. Therefore, a committee of the Brain Imaging Council of the Society of Nuclear Medicine was formed to address the need for specific guidelines regarding scan interpretation and reporting. This committee considered the wide range of current and potential uses of PET and SPECT, including its growing role in forensics. A set of basic guidelines for the reporting and interpretation of brain imaging studies applicable to all clinical situations, including forensics, was formulated. These guidelines were composed in a manner sensitive to the need for standards that are scientifically defensible now, and which will continue to be valid as the field evolves. It is the intent of the committee and this summary document to positively influence the clinical use of brain SPECT and PET by offering guidance concerning the elements essential to a complete and useful clinical report, defining standards to differentiate well-established clinical applications from research uses and providing a framework in which to consider the appropriateness of functional brain imaging used in the forensic arena.

Key Words: PET; SPECT; clinical applications; forensics; guidelines

J Nucl Med 1996; 37:1256–1259

The use of SPECT and PET in the management of patients with stroke, epilepsy, brain tumors and dementia, and in some cases, movement disorders and moderate-to-severe head trauma is now well recognized (*1–9*). Scan abnormalities have also been identified in patients with certain psychiatric diagnoses, including depression, obsessive compulsive and panic disorders, schizophrenia and substance abuse (*10–19*), but consistent patterns for these disorders have not been confirmed. Sensitivity and specificity are often unknown and in many cases, group patterns may actually be too subtle to detect in individual patients.

More elusive or less well-characterized behavioral syndromes have also been studied (*20–29*). In many cases, the patterns are variable and not easily interpreted as being causally related to a particular disease entity (e.g., mild head injury, AIDS, chronic fatigue syndrome, toxic exposures, foreign-body reactions, autoimmune disorders, substance abuse, violence and others) (*30,31*). Furthermore, while specific PET and SPECT defects appear useful to confirm a certain disease diagnosis or to support the localization of a particular clinical finding (*32–35*), there is only limited evidence that specific diseases or neurological, psychiatric or behavioral deficits can be predicted from specific scan patterns (*36,37*). While these types of studies remain extremely important for identifying previously unrecognized brain abnormalities and potential disease mechanisms in a variety of neuropsychiatric illness, their utility in the management of individual patients is still far from clear.

As SPECT and PET become more widely available, enthusiasm tempered by a cautious attitude seems appropriate regarding their use in brain disorders as a whole, given clear evidence that functional patterns are highly dependent on a large number of technical, analytical and physiological variables. The purpose of this document is to provide recommendations and basic guidelines for brain SPECT and PET acquisition, interpretation and reporting, with particular attention to recognized and generally accepted clinical indications, and to urge caution regarding applications in unstudied behavioral disorders.

BASIC METHODOLOGICAL ISSUES

The Society of Nuclear Medicine has recently published technical guidelines on brain SPECT acquisition and image reconstruction (*38,39*). However, even with adherence to these recommendations, the quality of the study will vary from institution to institution and is dependent on several factors, including instrumentation, collimation, filters, behavioral state of the subject during tracer uptake, timing of the scan relative to tracer injection, scan duration, patient movement, attenuation, reconstruction and analytical methods, as well as quality control.

In general, disease patterns are established using specific instruments, physiological measurements and methods of analysis. However, for some situations, the imaging technology available at a particular site may not be sufficient for diagnostic purposes. Accordingly, the degree to which subsequent studies

Received Mar. 12, 1996; accepted Mar. 20, 1996.
For correspondence or reprints contact: Joanna Wilson, Council Coordinator, Society of Nuclear Medicine, 1850 Samuel Morse Dr., Reston, VA 22090.